Response to Reviewer 3

Reviewer 3# comments

Main points:

- Improving and completing the description of the CCN data analysis:
• The correction of the CN and CCN data for multiple charges and the transfer function is not trivial. The authors should either describe exactly how their data were corrected (e.g. in appendix, if not wished in the text) or at least reference the papers that describe the methods they used.
Response: A multiple charge correction and transfer function similar to that described in Deng et al. (2011) has been applied to each CN size distribution spectrum as well as to the CCN efficiency spectrum. As the reviewer suggested, the reference has been cited in the revised paper and added to the reference section:
Deng, Z., Zhao, C., Ma, N., Liu, F., Ran, L., Xu, W., Liang, Z., Liang, S., Huang, M., Ma, X., Zhang, Q., Quan, J., and Yan, P.: Size- resolved and bulk activation properties of aerosols in the North China Plain. Atmos. Chem. Phys., 11, 3835-3846, 2011.

• It is not always clearly distinguished between bulk and size-resolved CCN measurements. This could be easily done, e.g., by using different symbols and/or using distinct terms for the derived parameters (e.g. total CCN number concentration vs. CCN number concentration (measured behind the DMA, in size-resolved mode) and activation ratio vs. size-resolved activation ratio).
Response: As per the suggestion, we now use distinct terms to describe the parameters derived from bulk CCN measurements and size-resolved CCN measurements.

- Improving the Results section:
• The whole section on the CCN closure is totally inscrutable. It needs to be clarified which data sets exactly were used for which type of closure. I have read this section at least ten times and I still cannot figure out from the text which parameters are plotted in Figs. 5 and 6. I have done this kind of closure tests myself several times. Thus, I have an idea of what might be shown in the two figures but it is certainly not clearly described in the text. Also, because the method is not described properly, it is hard to understand what the results tell us. Therefore the description of the method as well as the discussion of the closure results needs to be revised.

The parameters I would calculate and compare with each other for your study would be the following:
a. The actually measured total CCN concentration directly measured by the CCNC.
b. The observed total CCN concentration obtained from size-resolved CCN measurements: the actually measured CCN efficiency spectrum is multiplied by the actually measured CN size distribution, which yields the CCN size distribution; then this is integrated over the whole size range to obtain the total CCN concentration.
c. The predicted total CCN concentration obtained from the average CCN spectrum: the average measured CCN efficiency spectrum (would correspond to the spectra plotted in your Fig. 1) is multiplied by the actually measured CN size distribution, which yields the CCN size distribution; then this is integrated over the whole size range to obtain the total CCN concentration.
d. The predicted total CCN concentration obtained from the average CN size distribution: the actually measured CCN efficiency spectrum is multiplied by the average measured CN size distribution, which yields the CCN size distribution; then this is integrated over the whole size range to obtain the total CCN concentration.

The following comparisons of parameters would be interesting:
o a and b: This would be the easiest way to check if in general the size-resolved CCN measurements are consistent with bulk measurements. This comparison cannot be done in this study since no parallel bulk and size-resolved measurements are available.
Response: The reviewer is right. We may conduct such measurements in the future.

o b and c: For the time period of the size-resolved CCN measurements the total CCN concentration is 1) derived from the actually measured CCN spectrum and 2) calculated from the averaged CCN spectrum. With this comparison the influence of the variation of the chemical composition on the CCN concentration can be investigated, since the CN size distribution is the same for both the parameters. I guess this is what is shown in Fig. 5.
Response: The reviewer is right. Figure 5 in our study shows a comparison of "b" and "c", which is clearly described by the reviewer here. We call such a comparison a PO closure test, with the aim to investigate the influence of variations in chemical composition on CCN concentrations.

※a and c: For the time period when the bulk CCN measurements were

performed the measured total CCN concentration is compared with the calculated concentration from the averaged CCN spectrum. With this comparison again the variation of the chemical composition can be investigated but also how the bulk compares with the size-resolved CCN method. I guess this is what is shown in Fig. 6 but if so which average CCN spectra were then used for the calculation? The size-resolved CCN measurements, from which the CCN spectra can be derived, were made at different supersaturations than shown in Fig. 6.

Response: The reviewer is right. Figure 6 in our study shows a comparison of "a" and "c", which is clearly described by the reviewer here. We call such a comparison an NPO closure test. The reviewer asked which average CCN spectra were used for the estimation of CCN number concentration. This was not described clearly in the paper. The SS levels were set at 0.2%, 0.5%, and 0.8% when making the bulk CCN measurements. These values should be corrected as effective SS, thus they are are 0.23%, 0.51% and 0.80. The averaged CCN efficiency spectra at SS = 0.23% and 0.80% (Fig. 1) is directly used to estimate the total CCN concentration from 1-25 June. The mean CCN efficiency spectra at SS = 0.51% is calculated using the exponential relationships developed from plotting the three CDF fit parameters as a function of SS (R^2>0.90) (see the followingFigure).

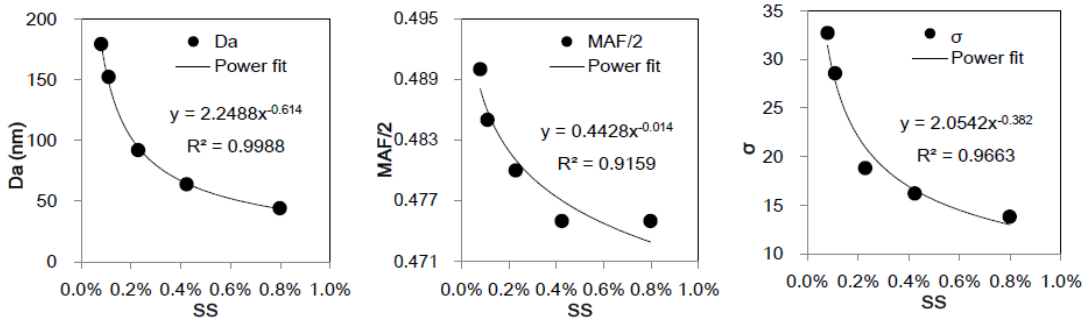

Fig. 1. D_a, MAF, and σ as a function of SS.

※ b and d: This comparison would be interesting for investigating the influence of the variation of the size distribution on the CCN concentration because here the CCN spectrum is the same for both the parameter. I guess that this reveals an even weaker correlation than for Fig. 6.

Response: As suggested by the reviewer, we plotted the comparison (see Fig. 2 below). Poor correlations are obtained, as expected by the reviewer. Particle size plays a key role in CCN activation, as shown in the literature. However, in this study, we mainly focus on investigating the influence of chemical composition on CCN activation. Also, in view of the current length of the paper, we prefer to not add

new material such as the suggested comparison.

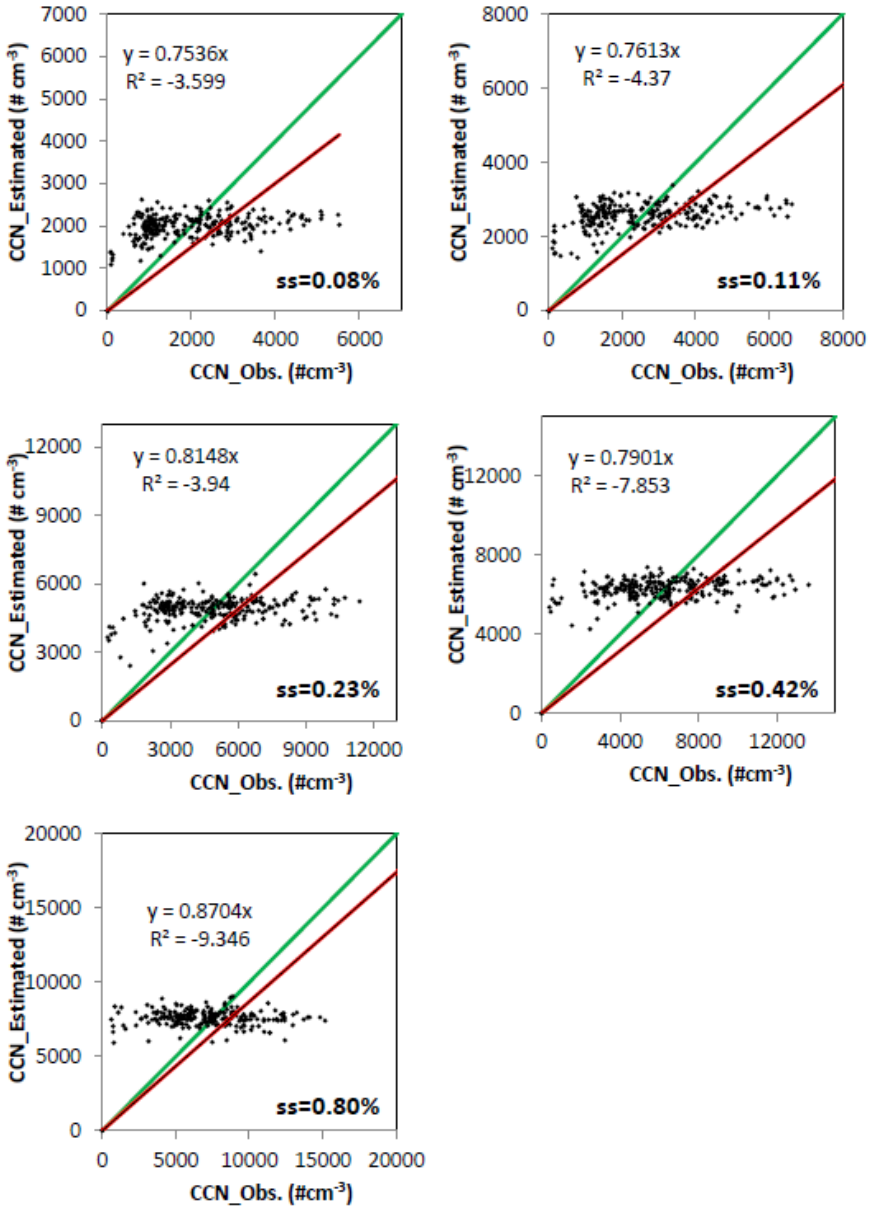

Fig. 2. Estimated N_{CCN} as a function of observed N_{CCN} in the parallel observation (PO) closure test (under the assumption of an unchanged particle size distribution). The green solid line is the 1:1 line.

Overall, the whole section on the CCN closure has been revised following the reviewer's comments and suggestions. Which data sets were used for which type of closure test has been stated in the revised paper.

• If MAF<1 is only due to an error of the CDF fit (p. 16, l.9-10), why the whole discussion on Da vs. Dcut is needed? It should be enough to report Da values only since Dcut is anyhow practically the same. Btw,

whether MAF<1 is an error of the CDF fit could be shown by plotting the data points in addition to the fit lines in Fig. 1!
Response: The discussion has been removed. The measured data points have been added to Fig. 1.

- Improving the presentation quality:
• The manuscript is written in bad English. In some cases, grammar mistakes even change the meaning of the sentence. Apart from that, the methods and results are not presented in a clear and well-structured way. While revising this manuscript you should make sure that "the description of experiments and calculations is sufficiently complete and precise to allow their reproduction by fellow scientists" (cf. ACP review aspects).
Response: The manuscript has been proofread by a native English speaker.

Specific remarks:

p. 2, l. 5-7: "A gradual increase…" This sentence is weird. I think what you mean is "A gradual increase of the activation ratio (AR) with particle diameter suggests that aerosol particles consisted of a variety of different hygroscopicities."
Response: The sentence has been corrected.

p.2, l.7-10: Better formulation: "During pollution events the activation diameter (Da) measured at low supersaturation (SS) was significantly increased compared to background conditions; the increase was not observed when SS>0.4%"
Response: Revised.
p. 4, l. 5: "aerosol particle formation" instead of "aerosol formation"
Response: Revised.
p. 4, l. 17: add "particle number" before "size distribution"
Response: Revised.
p. 5, l. 23-24: it must be "Rose et al., 2010; 2011; Gunthe et al., 2011" instead of "Rose et al., 2008; Gunthe et al., 2009"
Response: Corrected.
p. 7, l. 12-13: "Aerosol chemical composition…" I would shift this sentence to the end of this paragraph.
Response: Revised.

p. 8, l. 12: Which temperature sensor do you mean, inlet or sample temperature?
Response: Revised. It is the sample temperature.

p. 15, l. 15: Please give an error estimation for the supersaturation levels.
Response: Revised. The overall error (1σ) for the supersaturation levels is estimated to be < 3.5%.
p. 9, l. 22-23: What means "CCN data … were filtered according to the instrument recorded parameters"? Do you mean that you sorted the data? Did you throw out any data points? If so, explain why?
Response: Some data was discarded due to instrument fluctuations or malfunction. For example, if the relative difference between the actual and set sample flow is larger than 4%, the data are flagged as invalid data. If the "Temp. Stability" equaled "0", the data are also flagged as invalid data. These flagged data are not used in the analysis.

p. 10, l. 24: please add "of a particle" after "describe the ability"
Response: Revised.
p. 14, l. 16: it says that Fig.1 shows the "measured CCN efficiency", but this is not true. The figure shows the "CDF fit lines of the average CCN efficiency spectra". In fact, I would really appreciate if you could show the data points of the average spectra, too.
Response: Revised. The actual measured data points have been added.
p. 14, l. 21-23: "A gradual increase…". This is basically the same weird sentence as in the abstract. Please revise it according to my above suggestions.
Response: Revised.
p. 15, l. 1-2: Please reword this sentence: "The slope of AR around Da is less steep during polluted events than under background conditions, especially for low SS."
Response: It has been reworded as "The gentler slopes of AR around D_a during polluted events shows that the particle composition was more heterogeneous than the particle composition under background conditions."
p. 16, l. 5-7: "It should be noticed that… is equal to 1" I have no idea what these two sentences mean. Please revise.
Response: Revised.
p. 17, l. 18: change to "… may be due to the high amounts of organics freshly emitted…"
Response: Corrected.
p. 18, l. 18-19: I do not see that "Da_BG and Da_POL show larger variations at lower SS". Relatively seen, I would say that the largest variation is seen at SS = 0.11% and 0.23%. This would be also consistent with the variations for Da given in Tab. 1.
Response: Revised according to the reviewer's suggestion.

p. 21, l. 14-18: Here you discuss the correlation of AR at SS=0.2% with kappa_chem, which is also shown in Fig. 8a. However, Fig. 9, which you also refer to at this point, shows AR at SS=0.5%. Can you explain?
Response: Corrected. The SS in Fig. 9 has been changed to 0.23%.
p. 23, l. 16-20: "Based on the CDF fit method,… was not observed when SS>0.4%." These are the same strange sentence as in the abstract. Please see my comments above.
Response: The sentence has been revised.
p.23, l. 25: Rephrase as "However, the case is more complex for particles originating from heavy pollution…"
Response: Rephrased.
Tab. 1:
- Please indicate the meaning of the values in this table. Are they the arithmetic mean values +/- standard deviation over the entire measurement period?
Response: The values are arithmetic mean values ± one standard deviation.
- I think it would be sufficient to write only one digit after the comma for Da, Dcut, AR.
- Your MAF values decrease with increasing supersaturation. I think it makes physically no sense that all particles with ~ 300nm activate at SS=0.1% but not at 0.8%. If a particle is activated at SS=0.1% it is activated even more easily at 0.8%. Since the MAF values smaller than one seem to be an artifact, which you also mention on p. 16, l.9-10, the whole distinction between Da and Dcut is meaningless. In my point of view, in this manuscript, you should present the Da and respective kappa_a values only.
Response: The reviewer makes a good point. We have presented the D_a and respective kappa_a values only in the revised version of the manuscript.

Fig. 1:
- Please plot the data points of the average measured CCN efficiency spectra, too.
Response: Revised.
Fig. 2:
- Please indicate in the caption the meaning of the error bars and that this graph is depicting the size resolved CCN data.
- Btw., it would be also interesting to calculate the kappa from the bulk measurements.
Response: Revised. In the manuscript, kappa_chem, which represents the overall hygroscopicity of particles with particle sizes <1000 nm (PM1.0), was calculated from bulk chemical composition

measurements.
Fig. 4:
- What is plotted here? kappa_cut as mentioned in the caption or kappa_a as indicated in the x-axis label?
- I guess the particle size ranges as indicated in the individual panels should be consistent with the values of Tab. 1, but they are not.
Response: The typos have been fixed.

Fig. 7:
- Why do you write "AR (*100%)" in the y-axis labels? Is it not just the unitless AR that is plotted here?
- Please define the exact size ranges for the individual modes you integrated the particle number concentration (panel g, h).
- Please revise the figure caption. It is enough to write only once that the background conditions are plotted on the left and polluted conditions on the right.
Response: Revised.

Fig. 8:
- Please label the individual panels and indicate in the text accordingly.
Response: Revised.
- In fact, it would be also interesting to see ALL the combinations of AR (for all SS) versus kappa_chem, f44, and N_CN,Acc, N_CN,Ait, N_CN, Nuc; also the cases for which no good correlation is found. Therefore I suggest either to add panels for the other combinations or, what is probably more convenient, to add a table showing the correlation coefficients of all the combinations.
Response: We are currently working on another paper which will include such comparisons. We also plan to include data measured at several other sites. The manuscript underway aims to optimize CCN parameterization schemes in climate models.
Fig. 9: y-axis label: please remove "(*100%)". This is not valid, not for AR and especially not for kappa_chem.
Response: Revised.

Aerosol hygroscopicity and CCN activity during the AC^{3}Exp13 campaign: ~~implications~~Implications for CCN parameterization

~~F.~~Fang Zhang[1], ~~Z.~~Yanan Li[1], Zhanqing Li*[1,2], ~~Y. N. Li[1], L.~~Li Sun[3], ~~R.J.~~Runjun Li[1], ~~C.~~Chuanfeng Zhao[1], ~~P. C.~~Pucai Wang[3], ~~Y.L.~~Yele Sun[4], ~~X. G.~~Xinggang Liu[5], ~~J.X.~~Junxia Li[6, 7], ~~P. R.~~Peiren Li[6], ~~G.~~Gang Ren[6], ~~T. Y.~~Tianyi Fan[1]

[1]*College of Global Change and Earth System Science, Beijing Normal University, Beijing 100875, China*

[2]*Earth System Science Interdisciplinary Center and Department of Atmospheric and Oceanic Science, University of Maryland, College Park, Maryland, USA.*

[3]*Key Laboratory of Middle Atmosphere and Global Environment Observation (LAGEO), Institute of Atmospheric Physics, Chinese Academy of Sciences, Beijing, 100029, China*

[4]*State Key Laboratory of Atmospheric Boundary Layer Physics and Atmospheric Chemistry, Institute of Atmospheric Physics, Chinese Academy of Sciences, Beijing 100029, China*

[5]*State Key Laboratory of Water Environment Simulation, School of Environment, Beijing Normal University, Beijing 100875, China*

[6]*Weather Modification Office of Shanxi Province, Taiyuan, China, 030032*

[7]*Key Laboratory for Aerosol-Cloud-Precipitation of China Meteorological Administration , Nanjing University of Information Science and Technology, Nanjing,China,210044*

***correspondence to*: Z. Li (zli@atmos.umd.edu)**

Abstract

Aerosol hygroscopicity and cloud condensation nuclei (CCN) activity under background conditions and during polluted events are investigated during the Aerosol-CCN-Cloud Closure Experiment (AC^{3}Exp) campaign conducted at Xianghe, China in summer 2013. A gradual increase in size-resolved activation ratio (AR) ~~dependence on~~with particle diameter (D_p) suggests that aerosol particles ~~have lower hygroscopicity and heterogeneity of the composition during the campaign. Both~~ had different hygroscopicities. During pollution events, the activation diameter (D_a) ~~and cut-off diameter (D_{cut}) were increased~~ measured at low supersaturation (SS) was significantly ~~at lower super saturations (SS) (<0.2%) due~~increased compared to ~~pollutions (e.g. biomass burnings); the~~ background conditions. An increase was not observed when SS~~></~~ > 0.4%. ~~Hygroscopicity~~ The hygroscopicity parameter kappa (κ) ~~are about~~ was ~0.31-0.38 for particles in accumulation mode under background conditions~~ and about~~. This range in magnitude of κ is ~20% higher than ~~that~~κ derived under polluted conditions~~; however, κ are about 0.20-0.34 for~~. For particles in nucleation or Aitken mode ~~at~~, κ ranged from 0.20-0.34 for background ~~cases, showing slightly lower than that during~~and polluted ~~events~~cases. Larger particles were on average more hygroscopic than smaller particles. ~~But the case~~The situation is more complex for heavy pollution particles ~~with heavy pollutions due to the diversities~~because of the diversity in particle ~~compositions~~composition and mixing state. A non-parallel observation ~~(NPO)~~ CCN closure test ~~shows about 30%-40%~~ showed that uncertainties in ~~N_{CCN} prediction~~ CCN number concentration estimates

带格式的：字体颜色：黑色
带格式的：字体颜色：黑色
带格式的：字体颜色：黑色
带格式的：字体颜色：黑色
带格式的：字体颜色：黑色
带格式的：字体：Verdana，字体颜色：黑色

ranged from 30%-40%, which are associated with ~~the~~ changes ~~of~~in particle composition~~.~~ as well as measurement uncertainties associated with bulk and size-resolved CCN methods. A case study ~~shows~~showed that bulk CCN activation ~~ratio~~ratios increased ~~with the increase of~~as total condensation nuclei (CN) number concentrations (N_{CN}) ~~in~~increased on background days. ~~In the~~The case~~,~~ study also showed that bulk AR ~~exhibited good correlation~~correlated well with ~~κ_{chem}, which is~~the hygroscopicity parameter calculated from chemical volume fractions. On the contrary, bulk AR ~~declined~~decreased with ~~increase of~~increasing total N_{CN} during polluted events, but ~~it is~~was closely related to *f*44, which is usually associated with the particle organic oxidation level. Our study highlights the importance of chemical composition on determining ~~the particles~~particle activation properties~~, underlining~~ and underlines the significance of long-term ~~observation~~observations of CCN under different atmospheric environments, especially ~~those~~ regions with heavy ~~pollutions.~~

pollution.

1. Introduction

~~Indirect~~The indirect influence of aerosol particles on the radiative balance of the atmosphere through changes in cloud droplet number and the persistence of clouds (Twomey, 1974; Albrecht, 1989~~),~~) carries the largest uncertainty amongst the presently known causes of radiative forcing (IPCC, 2007, 2013). Thus, better understanding of aerosol particle formation, growth, and activation is essential.

Field and laboratory experiments have been conducted with the aim of better characterizing the particle physical and chemical parameters impacting on cloud condensation nuclei (CCN) activation. Studies have addressed the relative importance of the size distribution, particle composition, and mixing state in determining CCN activation, but there are disagreements on the relative importance of these parameters (e.g~~.~~, Roberts et al., 2002; Feingold, 2003; Ervens et al., 2005; Mircea et al., 2005; Dusek et al., 2006a; Anttila and Kerminen, 2007; Hudson, 2007; Quinn et al., 2008; Zhang et al., 2008; Deng et al., 2013, Ma et al~~.~~, 2013). CCN closure studies are a useful approach to test our knowledge of the controlling physical and chemical factors and to help verify experimental results. The CCN number concentration~~,~~ (~~—~~ (N_{CCN}~~,~~) is usually predicted from measured aerosol properties such as particle number size distribution and composition or hygroscopicity based on Köhler theory. The closure between the measured and estimated N_{CCN} is often ~~able to achieve in the~~achieved under background ~~atmosphere~~atmospheric conditions without heavy ~~pollutions~~pollution (Chuang et al., 2000; Dusek et al., 2003;VanReken et al., 2003; Rissler et al., 2004; Gasparini et al., 2006; Stroud et al., 2007~~;~~; Bougiatioti et al., 2009).

In urban/polluted areas, the particle size distribution is more complex ~~with various composition of air mass~~ (Lee et al., 2003; Alfarra et al., 2004; Zhang et al., ~~2004a~~2004;

Salcedo et al., 2006). ~~The particle~~Particle activation is affected by the composition and the mixing state of ~~the~~ aerosol particles. It has been demonstrated that particles are more difficult to ~~be activated~~activate during biomass burning ~~plumes~~plume events (Mircea et al., 2005; Lee et al., 2006; Clarke et al., 2007; Rose et al., 2010, 2011; Paramonov et al., 2013; Lathem et al., 2013). Also, their activation ratios ~~were~~are reduced by secondary organics formed from oxidation of common biogenic emissions (VanReken et al., 2005; Varutbangkul et al., 2006; Mei et al., 2013) and black carbon (Dusek et al., 2006b; Kuwata et al., 2007). Other organic components (e.g~~.~~., organic acids) ~~are~~have been shown to activate more easily (Raymond and Pandis, 2002; Hartz et al., 2006; Bougiatioti et al., 2011), but still much less than inorganic species. Therefore, ~~heavy polluted areas represent one of the most challenging cases to test~~testing the understanding of parameters controlling CCN activation and growth~~.~~ is challenging in heavily polluted areas. Furthermore, the main uncertainty in predicting the magnitude of ~~the~~ global aerosol indirect effects arises from those regions ~~with~~under the influence of urban emissions (Sotiropoulou et al., 2007). The study of aerosol-CCN closure and relationships ~~inside~~within and in the outflow of heavily polluted areas is thus important.

East Asia, especially the Jing (Beijing)-Jin (Tianjin)-Ji (Hebei) region, is a fast developing and densely populated region including numerous megacities, where anthropogenic aerosol emissions have increased significantly over recent years (Streets et al., 2008) and where aerosol loading is high and chemical composition is complex (Li et al., 2007a~~,~~; Xin et al., 2007). The high aerosol loading would have a significant influence on radiative properties, cloud microphysics, and precipitation (Xu, 2001; Li et al., 2007b; Xia et al., 2007; Rosenfeld et al., 2007; Lau et al., 2008; Li et al., 2011).

Field measurements of CCN have been made in East Asia where megacities are likely to be major sources of pollutants and CCN (Yum et al., 2007; Rose et al., ~~2008~~2010, 2011; Gunthe et al., 2009; Yue et al., 2011; Liu et al., 2011; Zhang et al., 2012; Deng et al., 2011; Leng et al., 2013). Despite the significant accomplishments achieved by these studies, limitations and uncertainties exist. As a recent example ~~for~~over the region of interest, Deng et al. (2011) over-~~-~~predicted ~~the concentration~~concentrations of CCN at a site in the North China Plain by 19% when compared with direct measurements.

The aim of this paper is to study ~~the~~ aerosol ~~hygroscopisity~~hygroscopicity and CCN activity under high aerosol loading ~~in the polluted regions, and get some implications~~conditions and to parameterize CCN number concentrations by using CCN activation ~~ratio~~ratios (AR) ~~to the~~as a proxy of the total number of aerosol particles in the atmosphere. ~~A~~ A cumulative Gaussian distribution function (CDF) fit model is applied to ~~both~~aerosol data collected under clean and polluted ~~aerosols~~conditions to ~~probe~~examine the ~~influences~~influence of size distribution, heterogeneity of chemical composition, and mixing state on CCN activity. The hygroscopicity parameter (κ) is derived using Köhler theory to study ~~aerosols~~aerosol hygroscopicity ~~during~~on clean days and during polluted events. In the CCN closure study, ~~besides~~in addition to the parallel observation (PO) closure test, we ~~employ~~apply the CCN efficiency spectrum to non-~~simultaneously~~ simultaneous condensation nuclei (CN) and bulk CCN ~~observation~~observations, namely the non-parallel observation (NPO) closure test, to estimate N_{CCN} ~~in order to test the impacts from particle composition.~~ Finally, the relationship between bulk AR and aerosol physical and chemical properties is examined ~~to imply a possibility of CCN parameterization in climate models.~~ .

2. ~~Measurement~~Measurements and data

An intensive field campaign~~, named~~ called the Aerosol-CCN-Cloud Closure Experiment (AC^{3}Exp~~),~~) was conducted during June and July of 2013 at the Xianghe Atmospheric Observatory (39.~~798N~~798°N, 116.~~958E~~958°E; 35 m above sea level~~),~~) located about 60 km southeast of the Beijing metropolitan area. This site is surrounded by agricultural land, densely occupied residences, and light industry. Sitting between two megacities (~~with~~ Beijing to the northwest and Tianjin to the southeast) and less than 5 km west of the local town center (with a population of 50,000), the site experiences frequent pollution plumes. Depending on the wind direction, instruments at the Xianghe site detect pollutants of urban, rural, or mixed origins, experiencing both fresh biomass burning emissions and advected aged aerosols. ~~More information~~Details about the measurement location and meteorological conditions ~~has been described by~~at the site can be found in Li et al. (2007, 2011).

带格式的：字体颜色：自动设置

2.1 ~~Instrument~~Instruments and ~~measurement~~measurements

~~In the campaign, bulk~~Bulk CCN activation was measured from 1 June to 25 June 2013. Size-resolved CCN ~~was~~were measured from 7 July to 21 July 2013.~~Aerosl~~ Aerosol particle size ~~distribution~~distributions (10-700 nm) ~~was~~were measured from 1 June to 25 June 2013 and from 7 July to 21 July 2013. During 1-25 June 2013, a Scanning Mobility Particle Sizer (SMPS) ~~(DMA; TSI 3081, CPC; TSI 3776)~~ was used independently for size distribution ~~measurement; and from~~measurements. From 7 July to 21 July 2013, it was combined with a Droplet Measurement Technologies - Cloud Condensation Nuclei Counter (DMT-CCNc) (Lance et al., 2006) and used for size-resolved CCN ~~measurement. Aerosol chemical composition was measured from~~

~~31 May to 30 June 2013. Therefore, the~~measurements. The CCN efficiency spectrum ~~(was Fig. 1) is~~ derived from ~~the~~ size-resolved CCN ~~observation~~observations made from 7 July to 21 July 2013. The aerosol particle size distribution data independently measured by the SMPS and bulk CCN measurements from 1 June to 25 June 2013 ~~combing~~combined with the derived CCN efficiency ~~spectra~~spectrum (Fig. 1) is used for the NPO CCN closure test. Aerosol chemical composition was measured from 31 May to 30 June 2013.

The aerosol inlet for the size distribution measurements was equipped with a TSI Environmental Sampling System (Model 3031200), which consists of a standard PM10 inlet, a sharp-cut PM1 cyclone, and a bundled nafion dryer. After dried through the nafion bundle, the sample flow with relative humidity (RH) of < 30% was sent into the SMPS for the aerosol size distribution measurements (10-700 nm). Meanwhile, the ~~CCN number concentrations (~~bulk N_{CCN}~~)~~ at different super-saturations ~~were~~(SS) was measured, using a continuous-flow CCN counter from the DMT-CCN_C. Each bulk CCN measurement cycle included three ~~supersaturations~~SS levels: 0.~~2~~23%, 0.~~5~~51% and 0.~~8~~80%. The scanning times for those ~~super-saturations~~SS levels were set ~~as~~at 7, 5, and 5 minutes, respectively.

The size-resolved CCN efficiency spectra were measured by coupling the same DMT-CCN_C used with the SMPS (Rose et al., 2008). In this setup the particles are rapidly dried with RH ~~of <~~< 30% upon entering the Differential Mobility Analyzer (DMA~~.~~). Thus, size selection is effectively performed under dry conditions, and the relative deviations in particle diameter should be < 1% except for potential kinetic limitations (Mikhailov et al., 2009). The sample flow exiting the DMA was split into two parts, with 0.3 lpm for the CPC and 0.5 lpm for the CCN_C. The DMA, controlled by the TSI-AIM software, scanned one size distribution every five minutes. The

带格式的: 字体: (国际) Times New Roman

CCN_C was operated at a total flow rate of 0.5 lpm with ~~the~~a sheath-to-aerosol flow ratio of 10. The inlet RH for CCN ~~is <~~was < 30%. During the field campaign, the ~~averaging~~mean sample temperature and pressure ~~as~~ measured by the CCN_C sensors were (23.5 ±1.6)~~ ~~℃ and (985.5 ± 3.6) hPa. The ~~deviations were determined by the measurement uncertainties. For~~SS levels of CCN_C were calibrated with ammonium sulfate before and after the field campaign, following procedures outlined in Rose et al. (2008). During each CCN measurement cycle, ~~SS was set to 5 different values:~~calibrated effective SS are 0.08~~;~~%, 0.11~~;~~%, 0.23~~;~~%, 0.42~~;~~%, and 0.80 ~~%.~~%. The overall error (1σ) for the SS levels was estimated to be < 3.5%. The completion of a full measurement cycle took 60 min (20 min for ~~the~~ SS = 0.08% and 10 min for ~~each of the rests). The supersaturations of CCN_C were calibrated with ammonium sulfate both before and after the campaign, following Rose's procedures (Rose et al., 2008).~~the other SS levels).

The measurement of non-refractory submicron ~~(NR-PM1)~~ aerosol species including organics, sulfate, nitrate, ammonium, and chloride were made with an Aerodyne Aerosol Chemical Speciation Monitor (ACSM) (Sun et al., 2012~~) is also conducted during the campaign.~~). The ACSM uses the same aerosol sampling, vaporization and ionization modules as the Aerosol Mass Spectrometer (AMS) (DeCarlo et al., 2006), but removes the size components~~, i.e., no size information.~~. During the field campaign, ambient ~~aerosol was~~aerosols were drawn inside through a ½ inch (outer diameter) stainless steel tube at a flow rate of ~3 L min^{-1}, of which ~84 cc min^{-1} was sub-sampled into the ACSM. An URG cyclone (Model: URG-2000-30ED) was also supplied in front of the sampling inlet to remove coarse particles with a size cut-off of 2.5 mm. Before sampled into the ACSM, aerosol particles are dried by Silica gel desiccant. The residence time in the sampling tube is ~5 s. The ACSM was operated at

带格式的

a time resolution of ~15 min with a scan rate of mass spectrometer at 500 ms amu^{-1} from m/z 10 to 150. Regarding the calibration of the ACSM, ~~the~~ mono-dispersed, size-selected 300 nm ammonium nitrate particles within a range of concentrations were sampled into both the ACSM and a condensation particle counter (CPC). The ionization efficiency (IE) was then determined by comparing the response factors of the ACSM to the mass calculated with ~~the~~ known particle size and ~~the~~ number concentrations from the CPC. Once the IE is determined, ~~the~~ changes ~~of~~in the internal standard naphthalene or air ions, e.g., m/z 28 (N_2^+) or m/z 32 ($O_2^{\pm}$~~)~~$^+$), can be used to account for the degradation of the detector. ~~The other~~Other details including the instrument, aerosol sampling setup, operations, and ~~calibrations were detailed~~calibration are given in Sun et al. (2012) and Ng et al. (2011).

In addition to the ACSM, the black carbon (BC) in PM2.5 was simultaneously measured at a time resolution of 5 min by a BC analyzer (Aethalometer, Model AE22, Magee Scientific Corporation). The campaign averaged mass concentrations of BC are ~4.2 μg m^{-3}, and the averaged mass fraction is about 6%, with maximum of 18% and minimum of 2%. During the experiment period, the campaign area was generally hot and ~~wet~~moist, with an average temperature of 23.6 ℃ and an average ambient ~~relative humidity (~~RH~~)~~ of 72.3%.

2.2 Data

The raw CCN data for both bulk and size-resolved CCN measurements were ~~firstly~~first filtered according to the instrument recorded parameters (e.g.~~.~~., temperature and flow). For example, if the relative difference between the actual and set sample flows was larger than 4%, the data are flagged as invalid data. If the "Temp. Stability" was recorded as "0", the data is also flagged as invalid data due to instrument

fluctuations. These flagged data are not used for further analysis. A multiple charge correction and transfer function (Deng et al., 2011) is applied ~~for~~to each CN size distribution spectrum as well as to the CCN efficiency spectrum. The CCN ~~activation ratio (~~AR~~)~~ is ~~just~~ the ratio of N_{CCN}/N_{CN}. ~~In order to~~To examine ~~the~~ CCN activity under different ~~cases, we classified~~ conditions, the size-resolved CCN efficiency data was classified as polluted ~~and~~or as background ~~conditions~~ based on the aerosol loading as well as the ~~synchronisms~~synchronal surface horizontal ~~winds~~wind data. ~~Basically, the polluted~~Polluted conditions are ~~with~~ identified when the total CN number concentration (N_{CN}~~>~~) > 15000 cm^{-3} and when the airflow came from southeast/east ~~and the background~~. Background cases are ~~with~~identified when N_{CN} < 15000 cm^{-3} ~~always associated with the~~and when winds were from the west or northwest. N_{CN} is the total aerosol number ~~concentrations~~concentration with a particle size range of 10-700 nm. Here, the background refers to a regional background condition which represents a well-mixed atmosphere ~~without influenced~~unaffected by local emissions, e.g.~~,~~ biomass burning. Bulk ~~measurement~~measurements of total CCN number concentrations at SS levels of 0.2%, 0.5% and 0.8% could lead to a considerable underestimation of ~~CCN~~N_{CCN} under polluted conditions (Deng et al., 2011) due to water depletion inside the column (Lathem and Nenes, 2011). Therefore, in this study ~~the,~~ data points with N_{CN} > 25000 cm^{-3} were excluded. In the closure study, CCN size distributions were calculated by multiplying the fitted campaign-averaged CCN efficiency ~~spectra (~~spectrum (a 3-parameter CDF fit) with the aerosol particle number size distribution. ~~Total~~The total N_{CCN} was then obtained by integrating the ~~CCN~~size-resolved N_{CCN} over the whole size range. ~~The~~Aerosol mass concentrations ~~and mass spectra~~ were processed using ACSM standard data analysis software (~~v~~version 1.5.1.1). ~~The detailed~~Detailed procedures for the data analysis have been

described in Ng et al. (2011) and Sun et al. (2012). ~~The campaign averaged mass concentrations of BC are ~4.2 μg m^{-3}, and the averaged mass fraction are about 6%, with maximum of 18% and minimum of 2%.~~

3. Theory

As proposed by Petters and Kreidenweis (2007), κ can be used to describe the ability of particles to absorb water vapor and act as CCN. Based on Köhler theory (Köhler, 1936), κ relates the dry diameter of aerosol particles to the critical water vapor SS. According to measurements and thermodynamic models, κ is zero for insoluble materials like soot or mineral dust~~, however~~. However, their hygroscopicity ~~would be changed~~changes due to the aging process ~~of the soot and mineral dust and~~, so the κ value then is ~~thus ~~> 0. The magnitude of κ is 0.1 for secondary organic aerosols, 0.6 for ammonium sulfate and nitrate, 0.95-1 for sea salt (Niedermeier et al., 2008), and 1.28 for sodium chloride aerosols. The effective hygroscopicity of mixed aerosols can be approximated by a linear combination of the κ-values of the individual chemical components weighted by the volume or mass fractions~~, respectively~~ (Kreidenweis et al., 2008; Gunthe et al., 2009). In this study, we calculated κ based on both size-resolved CCN measurements and bulk chemical composition observations made during the field campaign. The method to ~~derived~~derive κ is described below.

3.1 Derivation of κ_a ~~and κ_{cut}~~

~~Particle hygroscopicity~~The magnitude of κ ~~were~~was derived from the measured size -resolved CCN activated fraction using κ-Köhler theory (Petters and Kreidenweis, 2007). In κ-Köhler theory, the water vapor saturation ratio over an aqueous solution droplet S is given by:

$$S = \frac{D^3 - D_p^3}{D^3 - D_p^3(1-\kappa)} \exp\left(\frac{4\sigma_w M_w}{RT\rho_w D}\right) , \quad (1)$$

where D is the droplet diameter, D_p is the dry diameter of the particle, M_w is the molecular weight of water, σ_w is the surface tension of pure water, ρ_w is the density of water, R is the gas constant, and T is the absolute temperature. When κ is greater than 0.1, it can be conveniently ~~derived~~expressed as:

带格式的：字体：非倾斜

带格式的：字体：非倾斜

$$\kappa = \frac{4A^3}{27D_p^3 S_c^2} \quad (2)$$

$$A = \frac{4\sigma_w M_w}{RT\rho_w} , \quad (3)$$

where S_c is the particle critical supersaturation and is derived using the approach described by Rose et al~~.~~, (2008). The characteristic S_c of the size selected CCN is represented by the ~~supersaturation~~SS level at which AR reaches 50%. For the parameters listed above, T = 298.~~15K~~15 K, R~~=~~ = 8.315 J K^{-1} mol^{-1} ~~(gas constant),~~ ρ_w ~~=~~ = 997.1 kg m^{-3}, M_w ~~=~~ = 0.018015 kg mol^{-1}, and σ_w ~~=~~ = 0.072 ~~Jm~~J m^{-2}. Note that values derived from CCN measurement data through Köhler model calculations assuming the surface tension of pure water have to be regarded as "effective hygroscopicity parameters" that account not only for the reduction of water activity by the solute ("effective Raoult parameters") but also for surface tension effects (Petters and Kreidenweis, 2007).

In this study, a parameter called κ_a, which characterizes the average hygroscopicity of CCN-active particles in the size range around activated diameters (D_a), is calculated from the data pairs of SS and D_a based on the κ-Köhler theory. ~~Similarly, a parameter κ_{cut} is also derived from the data pairs of SS and a critical dry particle diameter (D_{cut})~~

~~based on the κ-Köhler theory, which characterizes the average hygroscopicity of aerosol particles in the size range around D_{cut}. Note the D_{cut} is the diameter when the AR=50% regardless of maximum activation fraction (MAF) smaller than 1 or equal to 1. Whereas, D_a is the diameter when the AR=MAF/2. The discrepancy of D_{cut} and D_a can reflect the mixing state and chemical heterogeneity of aerosol particles.~~

带格式的：字体颜色：文字 1

3.2 Derivation of κ_{chem}

For a given internal mixture, κ can be predicted by a simple mixing rule on the basis of chemical volume fractions, ε_i (Petters and Kreidenweis, 2007; Gunthe et al., 2009~~).~~):

$$\kappa_{chem} = \sum_i \varepsilon_i \kappa_i \quad , \qquad (4)$$

where~~,~~ κ_i and ε_i are the hygroscopicity parameter and volume fraction for the individual (dry) ~~component~~components in the mixture ~~with~~and i is the number of components in the mixture. We derive ε_i from the particle chemical composition measured by the ACSM. Measurements from the ACSM show that the composition of submicron particles was dominated by organics, followed by nitrate, ammonium, and sulfate. The contribution of chloride was negligible (with a volume fraction of about < 2%). The analysis of the anion and cation balance suggests that anionic species (NO_3^-, SO_4^{2-}) were essentially neutralized by NH_4^+ over the relevant size range. For refractory species, BC represented a negligible fraction of the total submicron aerosol volume (less than ~~about~~ 3%). ~~The sea~~Sea salt and dust are usually ~~with~~ coarse mode particles with particle ~~size of~~>sizes > 1 ~~μ~~μm (Whitby, 1978~~), the~~). The contribution of such types of aerosols ~~are~~is thus expected to be negligible for ~~the size range of~~ <sizes < 1000 nm. Therefore, ~~those~~the submicron particles measured by the ACSM

带格式的：字体：非倾斜

~~were~~ mainly ~~consisting~~consisted of ~~Organics~~organics, $(NH_4)_2SO_4$, and NH_4NO_3. The particle hygroscopicity is thus the volume average of the three participating species:

$$\kappa_{chem} = \kappa_{Org}\,\varepsilon_{Org} + \kappa_{(NH4)2SO4}\,\varepsilon_{(NH4)2SO4} + \kappa_{NH4NO3}\,\varepsilon_{NH4NO3}, \quad (5)$$

The values of κ are 0.67 and 0.61 for $(NH_4)_2SO_4$ and NH_4NO_3, respectively, and are derived from previous laboratory experiments (Petters ~~et al.,~~and Kreidenweis, 2007). ~~For Organics, we used a~~The following linear function ~~between κ_{Org} and f_{44}~~ derived by Mei et al.~~,~~ (2013) was used to estimate ~~the~~ κ_{Org} in our study~~. The formula is written as:~~

$$\kappa_{Org} = 2.10 \times f_{44} - 0.11$$

~~(Mei et al., 2013). By applying the function, calculated κ_{Org}.~~ The mean value of κ_{Org} during the field campaign is 0.115 ± 0.019 ~~during the observed period~~. Species volume fractions were derived from mass concentrations and densities of participating species. The densities of $(NH_4)_2SO_4$ and NH_4NO_3 are 1770 kg m^{-3} and 1720 kg m^{-3}, respectively. ~~And the~~The density of organics is 1200 kg m^{-3} (Turpin et al., 2001).

带格式的: 字体: MPHV

带格式的: 字体: MPHV

带格式的: 非上标/ 下标

4. Results and discussion

4.1 CDF fit and parameters derived from the CCN efficiency

The spectra of measured CCN efficiency ~~at~~under both polluted and background conditions were fitted with a ~~cumulative Gaussian distribution function (~~CDF~~;~~ (Rose et al., 2008):

$$f_{N_{CCN}/N_{CN}} = a\left(1 + \mathrm{erf}\left(\frac{D - D_a}{\sigma_a\sqrt{2}}\right)\right), \quad (6)$$

where~~,~~ the maximum activated fraction, MAF~~=~~, is equal to 2a, D_a is the midpoint activation diameter~~ D_a~~, and σ_a is the CDF standard deviation~~ σ_a. The~~. These parameters were determined for each spectrum. If MAF=1 by changing the parameter "a" to 0.5, the spectrum is characteristic for internally mixed aerosols with

homogeneous composition and hygroscopicity~~ of the particles.~~. The 3-parameter fit results represent the average activation properties of the aerosol particle fraction. During the field campaign~~ period of AC^{3}Exp 2013, we measured~~, about 1200 size-resolved CCN efficiency spectra for atmospheric aerosols at SS levels of 0.08% to 0.80~~%. Fig.~~% were measured. Figure 1 shows campaign-averaged spectra of both measured and fitted CCN efficiency at SS levels of 0.08%, 0.11%, 0.23%, 0.42~~%~~%, and 0.80% for background and polluted conditions. The slope of AR with respect to ~~diameter~~diameters near D_a in Fig. 1 provides information ~~on~~about the heterogeneity of the composition for the size~~—~~-resolved particles. For an ideal case when all CCN-active particles have the same composition and size, a steep change of AR from 0 to MAF would be observed as D reaches D_a. A gradual increase in size-resolved AR with particle diameter suggests that ~~some of the~~aerosol particles ~~have lower hygroscopicity and/or heterogeneity of the composition and are not able to activate at the given SS than others.~~consisted of different hygroscopicities. The ~~slope~~gentler slopes of AR around D_a during polluted events ~~shows gentler increase compared with those~~show that the particle composition was more heterogeneous than the particle composition under background conditions~~, especially at low SS. Overall, significant~~. Significant differences ~~of the~~in size-resolved CCN efficiency spectra ~~for~~under polluted and clean conditions at lower SS levels have been derived. The different ~~shape just suggests aerosols hygroscopisity and~~shapes suggest that aerosol hygroscopicity and CCN activity would be affected by ~~the~~ local emission sources~~ (~~, e.g.~~.~~, biomass burning~~).~~.

~~The three parameters (MAF, D_a, and σ) of CCN efficiency spectra derived from the 3-parameter CDF fits as well as D_{cut}, κ_a and κ_{cut} under polluted and clean conditions were also summarized in Table 1. Da_POL and Da_BG in Table 1 are defined as~~

~~activation diameter under polluted and clean conditions respectively. Dcut_POL and Dcut_BG are defined as cut-off diameter under polluted and clean conditions respectively.~~

4.1.1 Activation diameter (D_a)

The three parameters (MAF, D_a, and σ) describing the CCN efficiency spectra derived from the 3-parameter CDF fits, as well as κ_a under polluted and clean conditions, are summarized in Table 1. Activation diameters under polluted and clean conditions are denoted as Da_POL and Da_BG in Table 1, respectively. As expected, D_a ~~decreased~~decreases with increasing SS under both background and polluted conditions. At a given SS, D_a_POL ~~are larger~~is greater than D_a_BG~~. That means the~~, suggesting that particles ~~at~~under polluted ~~cases~~conditions would be activated at a larger diameter. ~~But~~As SS increases, the difference ~~of D_a_POL and D_a_BG reduced and was close to each other with the increasing of SS. Accordingly, D_{cut}~~between D_a_POL and ~~D_{cut}~~D_a_BG ~~dependence on SS showed similar changes to D_a. But, as stated previously, D_{cut} shows a little bit larger than D_a. Because D_{cut} is defined as the diameter when AR is up to 50%, but based on the CDF fit, the "MAF/2" is smaller than 50% and thus results in a smaller D_a.~~ decreases.

带格式的

4.1.2 Maximum Activated Fraction (MAF)

~~Generally~~In general, aerosols with a more uniform and homogenous chemical composition or with a core-shell structure would have a higher MAF. ~~MAF_POL and MAF_BG in Table 1 are defined as maximum activation fraction~~The MAF under polluted and background conditions is denoted by MAF_POL and MAF_BG in Table 1, respectively ~~the~~. Values of MAF_BG and MAF_POL ~~are~~range from 0.95-0.98 and

from 0.94-0.98, respectively~~ at different SS.~~. No significant discrepancies ~~of~~in MAF ~~were~~are observed between polluted and background conditions~~. It should be noticed that MAF are just closer to 1 but equal to 1. Because MAF for pure ammonium sulphate particles (0.05mol L^{-1}) is equal to 1; Furthermore, the observations have indicated~~ Observations show that particles can ~~be able to~~ activate to CCN completely when particle ~~diameter >~~diameters are greater than 300 nm even at SS~~=~~ = 0.08%. ~~Therefore,~~ This suggests that a smaller portion ~~(~~of 1−MAF~~,~~ (2-6%) is ~~just~~ caused by the error ~~of~~in the CDF fit, which will lead to a lower MAF than ~~it should be~~expected.

4.1.3 CDF standard deviations (σ)

~~The~~ CDF standard deviations (σ) are general indicators for the extent of external mixing and the heterogeneity of particle composition for ~~the investigated aerosol~~aerosols in the size range around D_a. ~~σ_POL and σ_BG in Table 1 are defined as~~ CDF ~~standard deviations~~σ under polluted and background conditions are denoted as σ_POL and σ_BG in Table 1, respectively. Under ideal conditions, ~~the CDF standard deviations should be~~σ equals zero for an internally mixed, fully mono-~~disperse~~dispersed aerosol with particles of homogeneous chemical ~~compositions~~composition. According to Rose et al.~~(~~. (2008), even after correcting for the DMA transfer function~~, however~~, calibration aerosols composed of high-purity ammonium sulfate exhibit small non-zero σ values that correspond to ~3% of D_a. ~~It~~This can be attributed to heterogeneities of the water vapor SS profile in the CCNC or other non-idealities, such as DMA transfer function and particle shape effects. Thus, "heterogeneity parameter" values of σ/D_a~~=~~ = 3% indicate internally mixed CCN, whereas higher values indicate external mixtures of particles. ~~σ/Da_POL and σ/Da_BG in Table 1 are defined as heterogeneity parameter~~Heterogeneity parameters

under polluted and background conditions are denoted as σ/Da_POL and σ/Da_BG in Table 1, respectively. ~~According to Table 1, σ /D$_a$_POL and σ /D$_a$_BG are with values of~~They range from 17%-30%, which is much higher than the 3% observed for pure ammonium sulfate, indicating that the particles were externally mixed with respect to their solute content.

4.2 Derived κ_a dependence on D_a

~~Fig.~~Figure 2 shows the dependence of κ_a on D_a under ~~both~~ background and polluted conditions. κ_a_POL~~—~~ and κ_a_BG are defined as the average hygroscopicity of CCN-active particles in the size range around D_a under polluted and background conditions~~.~~, respectively. For background days, larger particles were on average more hygroscopic than smaller particles~~:~~, i.e., κ_a_BG ~~increased~~increases substantially from about 0.22 at 30-60 nm to about 0.38 at the size range of 120-180 nm. ~~Our result~~This is consistent with ~~the~~ field results observed in Guangzhou, South China by Rose et al.~~,~~, (2010). However, compared to κ_a_BG, κ_a_POL ~~exhibited~~shows a relatively flat trend ~~with~~as the ~~increase of particles~~ particle size diameter~~. The κ_a_POL didn't exhibited significant increase but with larger~~ increases and error bars ~~around a given D$_p$, suggesting the complex and diversities of particle compositions~~are larger. This suggests that under polluted conditions, particle composition and their mixing state ~~at polluted cases.~~is complex and diverse. In this case, larger particles are even less hygroscopic than ~~the~~ smaller particles. One ~~of the~~ possible reason for ~~the~~ changes ~~of~~in κ_a ~~at~~under polluted ~~cases~~conditions may be ~~due to~~ the presence of high amount of organics freshly emitted from biomass burning (Andreae and Rosenfeld, 2008; Petters et al., 2009; Rose et al., 2010~~),~~) which would coat ~~on those~~the larger particles and ~~then lead the particles with~~render them less hygroscopic. Overall, κ for polluted

带格式的：字体颜色：黑色

aerosols are about 20% lower than that ~~of~~for clean aerosols for particles in the accumulation size range~~; for these~~. For particles in the nucleation or Aitken size range, κ_a for polluted particles is slightly higher than that ~~at~~for particles in the background cases. Based on laboratory ~~experiment~~experiments, Petters et al~~.~~,. (2009) examined the hygroscopic properties of particles freshly emitted from biomass burning. They found that κ was a function of particle size, with 250 nm particles being generally weakly hygroscopic and sub-100 nm particles being more hygroscopic. During the field campaign~~ at Xianghe, the~~, polluted cases represent cases where particles were mainly biomass burning aerosols~~ are the lead particles for the selected polluted cases.~~. The laboratory results, to some extent, can thus explain our field measurements. ~~But further~~Further investigations, including laboratory experiments and field measurements of size-resolved chemical composition, are needed to confirm and clarify this~~. The changes of κ_{cut}_POL and κ_{cut}_BG dependence on D_{cut}, which are not shown here, displayed similar characteristics. But the derived κ_{cut}_POL and κ_{cut}_BG (given in Table 1) are generally slightly smaller than κ_a_POL and κ_a_BG~~.

4.4 PDF of D_a and κ_a

~~Fig.~~Figure 3 ~~exhibits the~~shows probability distribution ~~function~~functions (PDF) of D_a under background conditions and during polluted events~~ throughout the campaign.~~. D_a_POL are mainly distributed in the ranges of about 185-205, 163-180, 95-120, 65-75 and 45-55 nm at SS levels of 0.08%, 0.11%, 0.23%, 0.42% and 0.80%, respectively. At each SS~~, PDF~~ level, the PDFs of D_a_POL ~~shows~~have a wider distribution than the PDFs of D_a_BG. ~~The PDF for D_a_POL moved several to dozens of nanometer and extended to~~At each SS level, the ~~side~~PDFs of D_a_POL extend to large particle ~~size at all SS~~ sizes indicating the impact by ~~pollutions. In addition, both~~

~~the~~ pollution. The largest variation in Da_BG and Da_POL ~~show larger variations at lower SS. This can be explained by two reasons: one~~ is ~~weaken~~seen at SS = 0.08% and 0.11%, respectively. One reason for this is the weakened impact ~~(solute effect)~~ of chemical composition on CCN activity at high SS~~;~~ levels, i.e., the solute effect. The other ~~one~~reason is ~~probably due to~~ the relatively larger uncertainties ~~for measuring lower~~that arise from making measurements at low SS levels.

~~Fig.~~Figure 4 ~~exhibits the PDF~~shows PDFs of κ_a under background conditions and during polluted events ~~throughout the campaign.~~. The PDF of κ_a_POL ~~presents~~has a large ~~variations~~variation at each size range around ~~D_a. At a given~~ D_p ~~range, they are distributed with~~and shows two modes. For example, κ_a_POL for particles around ~~the size diameter of~~ 48 nm ~~is with~~shows two ~~hygroscopic~~ peaks ~~of~~at ~0.15 and ~0.23~~; it is with peak~~. Peak values of ~0.26 and ~0.32 are seen for particles around D_p ~~=~~ = 198 nm. ~~Because a large amounts of κ_a are <0.3 but a very small portion of particles are with κ_a<0.1 at these cases. Such distribution mode for κ_a at polluted cases thus indicated an~~Most κ_a_POL values are less than 0.3. This suggests externally mixed, but ~~with~~ less hygroscopic particles during ~~the~~ polluted ~~cases. Compared to the PDF~~events. Less variation is seen in the PDFs of κ_a_POL, ~~κ_a_BC displays much less significant variations. It distributed with one~~BG. One mode ~~and~~is seen with peak values of 0.23, 0.30, 0.35, 0.35, and 0.38 ~~around the size diameter of~~for D_p = 46 ~~nm~~, 64 ~~nm~~, 92 ~~nm~~, 152 ~~nm~~, and 179 nm~~. Few particles are with κ_a<~~, respectively. Most κ_a_BG values are greater than 0.3 ~~at~~when D_p ~~></~~ > 60 nm ~~under background conditions, reflecting~~, indicating that the particles are more hygroscopic with a relatively homogeneous composition ~~of the particles under background conditions~~.

带格式的: 字体: Times New Roman
带格式的: 非上标/ 下标
带格式的: 字体: Times New Roman
带格式的: 非上标/ 下标
带格式的: 下标

4.5 CCN closure tests

In this section, we compare observed total N_{CCN} ~~observations~~ with corresponding values that were estimated on the basis of aerosol particle number size distributions measured in parallel and ~~non-~~not in parallel and assuming a uniform ~~particles~~particle composition. ~~If the~~Closure is achieved if estimated and observed N_{CCN} agree quantitatively within the range of their ~~uncertainty,~~uncertainties.

4.5.1 PO closure ~~is achieved. By using averaged CDF fit curve method with an assumption of uniform chemical composition, CCN size distributions were firstly calculated by multiplying the CCN efficiency spectra with the total aerosol particle (CN) number size distributions measured in parallel and non-parallel. Estimated N_{CCN} were calculated by stepwise integration of the CCN size distributions from 10 to 700 nm.~~ test

In PO closure tests, the measured CCN efficiency spectrum is first multiplied by the measured CN size distribution, which yields the CCN size distribution. This is then integrated over the whole size range to obtain the observed total CCN concentration (CCN_Obs). Size-resolved N_{CCN} are calculated by multiplying the campaign-averaged CCN efficiency spectrum with simultaneously measured CN number size distributions. Estimated total N_{CCN} (CCN_Estimated) are obtained by the stepwise integration of size-resolved N_{CCN} from 10 to 700 nm. With this comparison, the influence of the variation in chemical composition on the CCN concentration can be investigated because the CN size distribution is the same for both parameters.

Fig. ~~4.5.1 **Parallel observation (PO) closure tests**~~

~~The comparison of estimated and parallel observed N_{CCN}~~ 5 shows CCN_Estimated as a function of CCN_Obs. at ~~five~~ SS ~~of~~ levels ranging from 0.08% to 0.80~~% is shown in~~

带格式的: 字体: (国际) Times New Roman

~~Fig. 5. In this case, a good agreement between estimated~~%. Estimated and measured total N_{CCN} ~~was obtained~~agree well. The mean slope and correlation coefficient (R^2) are 0.99 and 0.97, respectively, at the five ~~super saturations. At~~ SS ~~of 0.08% and 0.11%, the results showed a little bit (~~levels. A ~3-4~~%)~~% underestimation ~~of CCN number concentrations.~~occurs at SS levels of 0.08% and 0.11%. One reason for ~~the~~this slight ~~worse closure between measured and estimated CCN number concentrations at lower SS lies in~~ underestimation is that size-resolved ~~activation ratios exhibit a larger variability~~ARs are more variable at low SS levels than ~~that~~ at higher SS levels. Also, compared to ~~the~~total activated CCN number concentrations at high SS~~, the N_{CCN} is with a~~ levels, there are less ~~amounts~~N_{CCN} at low SS levels, which would lead to larger uncertainties or to a lower correlation. Overall, ~~the~~ CCN closure can be achieved by using campaign-averaged CCN efficiency spectra. In this PO closure test ~~indicated that the estimation on a basis~~, the influence of ~~mean CDF fit AR curve methods can estimate the observed N_{CCN} pretty well when SS is high, although uniform and internally mixed~~variations in chemical composition ~~throughout the size range being assumed~~on CCN concentrations is insignificant.

4.5.2 ~~Non-parallel observation (~~NPO~~)~~ closure ~~tests~~test

~~In this study, we also~~Mean CCN efficiency spectra derived from size-resolved CCN measurements taken on 7-21 July 2013 are used to estimate total CCN number concentrations based on ~~non-parallel~~ CN size distribution measurements ~~(~~taken on 1-25 June~~, 2013)~~ 2013. This is referred to as an NPO closure test. The average measured CCN efficiency spectrum (corresponding to spectra in Fig. 1) is multiplied by the measured CN size distribution which yields the CCN size distribution. This is integrated over the whole size range (10-700 nm) to obtain the estimated total CCN

带格式的

带格式的

带格式的

带格式的

带格式的: 字体: 加粗

带格式的: 字体颜色: 黑色

concentration. The mean CCN efficiency spectra at SS levels of 0.23% and 0.80% (Fig. 1) is used to estimate the total CCN concentration during 1-25 June 2013. The mean CCN efficiency spectra at SS = 0.51% is derived using the exponential relationships developed from plotting the three CDF fit ~~curve derived from the size-resolved CCN measurements (7-21 July, 2013). The comparison of estimated~~ parameters as a function of SS (see Fig. 7).

Estimated total N_{CCN} ~~and the non-parallel~~ as a function of measured bulk N_{CCN} at SS levels of 0.~~2~~23%, 0.~~5%~~51%, and 0.~~8~~80% are shown in Fig. 6. ~~A reasonable agreement between estimated and measured N_{CCN} was obtained by using CDF fit curve method. The~~ The lower slope at SS~~= =~~ 0.~~2~~23% indicates that the estimation on ~~a~~the basis of NPO closure underestimates about 7% of the observed N_{CCN}. The closure is considerably improved at higher SS~~. However, only a~~ levels. A reasonable correlation ~~with R^2 of about 0.6-0.8~~ between estimated and measured total N_{CCN} ~~was achieved,~~is seen (R^2 = 0.6-0.8), which suggests temporal variations ~~both~~ in chemical composition ~~or~~and mixing state of aerosol particles. In addition, there are uncertainties due to measuring bulk and size-resolved CCN. Overall, ~~the~~ uncertainties in ~~such~~this NPO CCN closure study ~~are about~~range from 30%-40%. ~~Thus, it is important to conduct such field experiment to measure CCN under different environmental conditions. Likewise, caution needs to be exercised to use~~Caution is needed when using data from any ~~experiment of~~ short~~-periods~~-term experiment at a single site to do CCN ~~parameterization~~parameterizations for~~ any~~ large-scale applications. It is necessary to conduct long-term CCN measurements at more regional sites, especially those ~~with heavy pollution of high CN~~that are heavily polluted.

带格式的

带格式的：字体颜色：黑色

4.6 Case study: ~~implications of~~ CCN activation ~~combining~~and chemical composition

~~To understand the~~ The behavior of CCN activation under ~~different surrounding circumstance, two~~background and polluted conditions is examined. Two cases are selected: one case with total N_{CN} ~~<~~ < 15000 cm^{-3} ~~and >~~(background) and another case with total N_{CN} > 15000 cm^{-3} ~~during the campaign are selected for investigation, which are defined as background and polluted condition, respectively. Interestingly,~~ (polluted). Trends in bulk CCN activation ~~exhibits completely~~as N_{CN} increases are different ~~changes with N_{CN} from~~for the ~~two~~background and polluted cases~~: the~~. Bulk AR at ~~all~~the three SS ~~of~~ levels (0.~~2~~23%, 0.~~5%~~51%, and 0.~~8% increase with the increase of~~80%) increases as total N_{CN} ~~at~~increases for background cases (Fig~~. 7a), whereas they decline with increase of~~. 8a) and decreases as total N_{CN} ~~during~~increases for polluted ~~events~~cases (Fig~~. 7b). At~~. 8b). For the background cases, changes ~~of~~in bulk AR are ~~apparently dependence~~ dependent on changes ~~of~~in κ_{chem} (Fig. ~~7c), showing well~~8c). A good correlation between AR_0.~~2~~23 and κ_{chem} ~~with~~ (R^2 ~~></~~ > 0.7~~(~~) is seen in Fig. ~~8). Such~~9. A high ~~correlations~~correlation between bulk AR and κ_{chem} ~~have~~when total N_{CN} is low has been observed ~~when N_{CN} are low~~ during the ~~whole~~ campaign (Fig. ~~9~~10). In these cases, organics account for ~~relatively low amounts (~~~~~~30~~%)~~%~~ of the total particle mass ~~concentrations but~~concentration and concentrations of soluble inorganics are high (Fig. ~~7e~~8e). In particular, the mass concentration of nitrate is higher than that for organics ~~accounting~~and accounts for the largest mass fraction ~~of all compositions~~ when κ_{chem} reaches ~~the~~a maximum with a mean value of ~0.45. The *f*44, which is the fraction of total organic mass signal at *m/z* 44, is not correlated with AR (Fig. ~~7c~~8c). The *m/z* 44 signal is ~~due~~ mostly due to acids (Takegawa et al., 2007; Duplissy et al., 2011) or acid-derived species, such as esters,

and *f*44 is closely related to the organic oxidation level ~~(i.e., O:C ratio) (Aiken et al.,2008).~~ , i.e., O:C ratio (Aiken et al., 2008). Oxidized/aged acids are generally more hygroscopic and easily activated. Therefore, the lower correlation between *f44* and AR implies that organics under low N_{CN} conditions are less hygroscopic. CN number concentrations in the nucleation, Aitken, and accumulation modes are shown in Fig. 8g (polluted) and Fig. 8h (background). Under background conditions, bulk AR at SS = 0.23% is more correlated (R^2 = 0.5) with changes in N_{CN} in the accumulation mode (Fig. 9), suggesting that most aerosol particles with sizes > 100 nm can be activated. Smaller particles with Aitken diameters of < 40 nm at the given SS levels (0.23%-0.80%) are not as easily activated, if at all, so no correlation is seen (Fig. 8g). Under polluted conditions, there is little dependence of changes in bulk AR with changes in κ_{chem} (Fig. 8d). Bulk AR at SS = 0.23% is moderately correlated with *f*44 (R^2 = 0.5, Fig. 9). As stated above, *f*44 is always related to the organic oxidation level.

Usually, ~~the~~ oxidized/aged acids are more hygroscopic and easily activated. ~~Therefore, the deteriorated correlations between *f44* and AR implied that organics at low N_{CN} cases are less hygroscopic. In addition, CN number concentrations at size range of nucleation, Aitken and accumulated mode are also shown in Fig 7g and 7h for background and polluted conditions respectively. In background days, AR at SS=0.2% is more correlated with the changes of N_{CN} at accumulated mode with R^2 of ~0.5 (Fig. 8), suggesting aerosol particles at the size range of >100 nm can be mostly activated. Smaller particles with Aitken diameter of <40 nm at the given SS (0.2%-0.8%) are difficult or cannot be activated, thus there are no correlations indicated in Fig. 7g. During polluted events, changes of AR didn't displayed apparent dependence on changes of κ_{chem} (Fig. 7d). But AR at SS=0.2% showed moderate correlation with *f*44 with R^2 of ~0.5 (Fig. 8). As stated above, the *f*44 is always related to the organic~~

带格式的：字体：加粗

~~oxidation level. Usually, the oxidized/aged acids are more hygroscopic and easily activated.~~ The correlation between *f*44 and bulk AR ~~suggested~~suggests that the ~~significant roles of~~ organics ~~contributions~~contribution from oxidized or aged aerosols ~~to~~play a significant role in CCN activity~~. Because the impact from organics on the particles activation is complicated~~ (Jimenez et al., 2009). ~~In addition, it will introduce definite~~A bias is introduced by using a parameterized function derived from observations made at other sites with different aerosol types to describe the particle hygroscopicity and activation properties due to the complexity of the organic aerosol fraction and its tendency to evolve with atmospheric oxidative processing and aerosol aging ~~based on previous studies~~ (e.g.~~.~~., Padró et al., 2010; Engelhart et al., 2011, 2012; Asa-Awuku et al., 2011). ~~Similarly, under~~Under polluted conditions, the bulk AR_0.2 is more correlated with ~~the~~ changes ~~of accumulated~~in accumulation mode particles~~,~~ ~~with~~ (~~R^2 of~~= ~0.3~~.~~).

Overall, based on the case ~~investigation~~study, one cannot use a parameterized formula ~~combining with~~ using only total N_{CN} to estimate total CCN number concentrations. ~~However, if~~If observations such as size-resolve CCN ~~as well as~~and size-resolved chemical ~~compositions~~composition are not available, ~~a~~the possibility of using bulk κ_{chem} and *f*44 ~~by combining~~in combination with bulk N_{CN}~~>100nm~~ > 100 nm to parameterize CCN number concentrations ~~when with low and high N_{CN} respectively has been~~is implied~~. But further~~ by the case study. Further field investigations ~~or examinations~~ are needed to demonstrate and confirm the relationship between bulk AR and particle size and ~~compositions~~composition.

5. Summary and conclusions

Atmospheric aerosol particles acting as CCN are pivotal elements of the hydrological cycle and climate change. In this study, we measured and characterized ~~CCN~~N_{CCN} in

relatively clean and polluted air during the AC^{3}Exp campaign conducted at Xianghe, China during summer 2013~~, with the~~. The~~,~~ aim ~~of understanding the~~was to examine CCN activation properties under high aerosol loading conditions in ~~the~~a polluted ~~regions~~region and ~~implying~~to assess the impacts of particle size and chemical composition on the CCN ~~activation ratio to the~~ AR which acts as a proxy of the total number of aerosol particles in the atmosphere. Based on the CDF fit method, a gradual increase in ~~AR dependence on D_p~~size-resolved AR with particle diameter suggests that aerosol particles have ~~lower hygroscopicity and heterogeneity of the composition during the campaign. Both~~different hygroscopicities. D_a ~~and D_{cut} were~~ increased significantly at lower SS ~~(<~~levels (< 0.~~2~~23%) due to ~~pollutions (~~pollution, e.g~~.~~., biomass burnings~~); the~~. This increase was not observed when SS~~>~~ > 0.4%. ~~The value of κ are about 0.31-0.38 for~~For particles in the accumulation mode~~,~~, values of κ range from 0.31-0.38 under background conditions~~ and~~, which is about 20% higher than that derived under polluted conditions~~; however, κ are about 0.20-0.34 for~~. For particles in the nucleation or Aitken mode~~ at~~, κ range from 0.20-0.34 under both background ~~cases, showing slightly lower than that during~~ and polluted ~~events~~conditions. Larger particles were on average more hygroscopic than smaller particles. ~~But~~However, the case is more complex for particles ~~with~~originating from heavy ~~pollutions~~pollution due to the ~~diversities of~~diversity in particle ~~compositions~~composition and mixing state. ~~–~~The low R^2 for the NPO CCN closure test suggests ~~about~~a 30%-40% ~~uncertainties~~uncertainty in total N_{CCN} ~~prediction that is mainly caused by changes in particle composition. By combining analyses of~~ estimation. Using bulk chemical composition data from ACSM ~~measurement~~measurements, the relationship between bulk AR and the physical and chemical properties of ~~the~~ atmospheric ~~aerosol~~aerosols is investigated. Based on ~~the~~a

带格式的: 字体: Times New Roman

case ~~investigation~~study, we conclude that one cannot use a parameterized formula ~~combining with~~ using only total N_{CN} to estimate total N_{CCN}. We have ~~implied a~~shown the possibility of using bulk κ_{chem} and $f44$ ~~by combining~~in combination with bulk $N_{CN>100nm}$ > 100 nm to parameterize CCN number concentrations ~~when with low and high N_{CN} respectively~~. Further field investigations or examinations are needed to demonstrate and confirm the relationship between bulk AR and particle size and ~~compositions~~composition.

~~**Acknowledgement**~~

Acknowledgements

We ~~would~~ thank the ~~two~~ reviewers ~~very much~~ for their suggestions and comments which have greatly improved the paper. This work was funded by the National Basic Research Program of China '973' (Grant No. 2013CB955801, 2013CB955804), the National Science Foundation (1118325~~)~~), and the Fundamental Research Funds for the Central Universities (Grant No. 2013YB35). ~~The~~ We greatly appreciate the support of the entire AC^{3}Exp team ~~has been much appreciated~~.

带格式的: 字体: Calibri, 五号

References

Aiken, A. C., DeCarlo, P. F., Kroll, J. H., Worsnop, D. R., Huffman, J. A., Docherty, K. S., Ulbrich, I. M., Mohr, C., Kimmel, J. R., Sueper, D., Sun, Y., Zhang, Q., Trimborn, A., Northway, M., Ziemann, P. J., Canagaratna, M. R., Onasch, T. B., Alfarra, M. R., Prevot, A. S. H., Dommen, J., Duplissy, J., Metzger, A., Baltensperger, U., and Jimenez, J. L.: O/C and OM/OC ratios of primary, secondary, and ambient organic aerosols with high-resolution time-of-flight aerosol mass spectrometry, Environ. Sci. Technol., 42, 4478–4485, 2008.

Albrecht, B. A.: Aerosols, clouds and microphysics, Science, 245, 1227–1230, 1989.

Alfarra, M. R., Coe, H., Allan, J. D., Bower, K. N., Boudries, H., Canagaratna, M. R., Jimenez, J. L., Jayne, J. T., Garforth, A. A., Li, S.-M., and Worsnop, D. R.: Characterization of urban and rural organic particulate in the Lower Fraser Valley using two Aerodyne Aerosol Mass Spectrometers., Atmos. Environ., 38, 5745–5758, 2004.

Andreae, M. O. and Rosenfeld, D.: Aerosol-cloud precipitation interactions. Part 1. The nature and sources of cloud-active aerosols, Earth. Sci. Rev., 89, 13-41, doi:10.1016/j.earscirev.2008.03.001, 2008.

Anttila, T. and Kerminen, V. M.: On the contribution of Aitken mode particles to cloud droplet populations at continental background areas – a parametric sensitivity study, Atmos. Chem. Phys., 7, 4625–4637, 2007.

Asa-Awuku, A., Moore, R. H., Nenes, A., Bahreini, R., Holloway, J. S., Brock, C. A., Middlebrook, A. M., Ryerson, T., Jimenez, J., DeCarlo, P., Hecobian, A., Weber, R., Stickel, R., Tanner, D. J., and Huey, L. G.: Airborne cloud condensation nuclei measurements during the 2006 Texas Air Quality Study, J. Geophys. Res., 116, D11201, doi:10.1029/2010JD014874, 2011.

Bougiatioti, A., Fountoukis, C., Kalivitis, N., Pandis, S. N., Nenes, A., and Mihalopoulos, N.: Cloud condensation nuclei measurements in the marine boundary layer of the eastern Mediterranean: CCN closure and droplet growth kinetics. Atmos. Chem. Phys., 9, 7053–7066, 2009.

Bougiatioti, A., Nenes, A., Fountoukis, C., Kalivitis, N., Pandis, S. N., and Mihalopoulos, N.: Size-resolved CCN distributions and activation kinetics of aged continental and marine aerosol, Atmos. Chem. Phys., 11, 8791-8808, doi:10.5194/acp-11-8791-2011, 2011.

Chuang, P. Y., Collins, D. R., Pawlowska, H., Snider, J. R., Jonsson, H. H., Brenguier,

J. L., Flagan, R. C., and Seinfeld, J. H.: CCN measurements during ACE-2 and their relationship to cloud microphysical properties, Tellus B, 52, 843–867, 2000.

Clarke, A., McNaughton, C., Kasputin, V. N., Shinozuka, Y., Howell, S., Dibb, J., Zhou, J., Anderson, B., Brekhovskikh, V., Turner, H., and Pinkerton, M.: Biomass burning and pollution aerosol over North America: Organic components and their influence on spectral optical properties and humidification response, J. Geophys. Res., 112, D12S18, doi:10.1029/2006JD007777, 2007.

DeCarlo, P.F., Kimmel, J.R., Trimborn, A., Northway, M.J., Jayne, J.T., Aiken, A.C.,Gonin, M., Fuhrer, K., Horvath, T., Docherty, K.S., Worsnop, D.R., Jimenez, J.L.: Field-deployable, high-resolution, time-of-flight aerosol mass spectrometer. Anal. Chem., 78, 8281-8289, 2006.

Deng, Z., Zhao, C., Ma, N., Liu, F., Ran, L., Xu, W., Liang, Z., Liang, S., Huang, M., Ma, X., Zhang, Q., Quan, J., and Yan, P.: Size- resolved and bulk activation properties of aerosols in the North China Plain. Atmos. Chem. Phys., 11, 3835-3846, 2011.

Deng, Z., Zhao, C., Ma, N., Ran, L., Zhou, G., Lu, D., and Zhou, X.: An examination of parameterizations for the CCN number concentration based on in situ measurements of aerosol activation properties in the North China Plain, Atmos. Chem. Phys., 13, 6227–6237, doi:10.5194/acp-13-6227-2013, 2013.

Dusek, U., Covert, D. S., Wiedensohler, A., Neususs, C., Weise, D., and Cantrell, W.: Cloud condensation nuclei spectra derived from size distributions and hygroscopic properties of the aerosol in coastal south-west Portugal during ACE-2, Tellus B, 55, 35–53, 2003.

Dusek, U., Frank, G. P., Hildebrandt, L., Curtius, J., Schneider, J., Walter, S., Chand, D., Drewnick, F., Hings, S., Jung, D., Borrmann, S., and Andreae, M. O.: Size

带格式的: 字体: Times New Roman

matters more than chemistry for cloud-nucleating ability of aerosol particles, Science, 312, 1375–1378, 2006a.

Dusek, U., Reischl, G. P., and Hitzenberger, R.: CCN activation of pure and coated carbon black particles, Environ. Sci. Technol., 40, 1223–1230, 2006b.

Duplissy, J., DeCarlo, P. F., Dommen, J., Alfarra, M. R., Metzger, A., Barmpadimos, I., Prevot, A. S. H.,Weingartner, E., Tritscher, T., Gysel, M., Aiken, A. C., Jimenez, J. L., Canagaratna, M. R., Worsnop, D. R., Collins, D. R., Tomlinson, J., and Baltensperger, U.: Relating hygroscopicity and composition of organic aerosol particulate matter, Atmos. Chem. Phys., 11, 1155–1165, doi:10.5194/acp-11-1155-2011, 2011.

Engelhart, G. J., Moore, R. H., Nenes, A., and Pandis, S. N.: Cloud condensation nuclei activity of isoprene secondary organic aerosol, J. Geophys. Res., 116, D02207, doi:10.1029/2010JD014706, 2011.

Engelhart, G. J., Hennigan, C. J., Miracolo, M. A., Robinson, A. L., and Pandis, S. N.: Cloud condensation nuclei activity of fresh primary and aged biomass burning aerosol, Atmos. Chem. Phys., 12, 7285–7293, doi:10.5194/acp-12-7285-2012, 2012.

Ervens, B., Feingold, G., and Kreidenweis, S.: Influence of watersoluble organic carbon on cloud drop number concentration., J. Geophys. Res., 110, D18211, doi:10.1029/2004JD005634, 2005.

Feingold, G.: Modeling of the first indirect effect: Analysis of measurement requirements, Geophys. Res. Lett., 30(19), doi:10.1029/2003GL017967, 2003.

Gasparini, R., Collins, D. R., Andrews, E., Sheridan, P. J., Ogren, J. A., and Hudson, J. G.: Coupling aerosol size distributions and size-resolved hygroscopicity to predict humidity-dependent optical properties and cloud condensation nuclei spectra., J.

Geophys. Res., 111, D05S13, doi:10.1029/2005JD006092, 2006.

Gunthe, S. S., King, S. M., Rose, D., Chen, Q., Roldin, P., Farmer, D. K., Jimenez, J. L., Artaxo, P., Andreae, M. O., Martin, S. T., and Pöschl, U.: Cloud condensation nuclei in pristine tropical rainforest air of Amazonia: size-resolved measurements and modeling of atmospheric aerosol composition and CCN activity, Atmos. Chem. Phys., 9, 7551-7575, doi:10.5194/acp-9-7551-2009, 2009.

Hartz, K. E. H., Tischuk, J. E., Chan, M. N., Chan, C. K., Donahue, N. M., and Pandis, S. N.: Cloud condensation nuclei activation of limited solubility organic aerosol, Atmos. Environ., 40, 605–617, 2006.

Hudson, J.: Variability of the relationship between particle size and cloud-nucleating ability, Geophys. Res. Lett., 34, L08801, doi:10.1029/2006GL028850, 2007.

IPCC: Climate change 2007: Scientific basis, Fourth assessment of the Inter-governmental Panel on Climate Change, Cambridge Univ. Press, New York, 2007.

IPCC: Climate change 2013: Scientific basis, Fifth assessment of the Inter-governmental Panel on Climate Change, Cambridge Univ. Press, New York, 2013.

Jimenez, J. L., Canagaratna, M. R., Donahue, N. M., Prevot, A. S. H., Zhang, Q., Kroll, J. H., DeCarlo, P. F., Allan, J. D., Coe, H., Ng, N. L., Aiken, A. C., Docherty, K. S., Ulbrich, I. M., Grieshop, A. P., Robinson, A. L., Duplissy, J., Smith, J. D., Wilson, K. R., Lanz, V. A., Hueglin, C., Sun, Y. L., Tian, J., Laaksonen, A., Raatikainen, T., Rautiainen, J., Vaattovaara, P., Ehn, M., Kulmala, M., Tomlinson, J. M., Collins, D. R., Cubison, M. J., Dunlea, E. J., Huffman, J. A., Onasch, T. B., Alfarra, M. R., Williams, P. I., Bower, K., Kondo, Y., Schneider, J., Drewnick, F., Borrmann, S., Weimer, S., Demerjian, K., Salcedo, D., Cottrell, L., Griffin, R.,

Takami, A., Miyoshi, T., Hatakeyama, S., Shimono, A., Sun, J. Y., Zhang, Y. M., Dzepina, K., Kimmel, J. R., Sueper, D., Jayne, J. T., Herndon, S. C., Trimborn, A. M., Williams, L. R., Wood, E. C., Middlebrook, A. M., Kolb, C. E., Baltensperger, U., and Worsnop, D. R.: Evolution of Organic Aerosols in the Atmosphere, Science, 326, 1525–1529, 2009.

Köhler, H.: The nucleus in and growth of hygroscopic droplets, Trans. Faraday Soc., 32, 1152–1161, doi:10.1039/TF9363201152, 1936.

Kreidenweis, S. M., Petters, M. D., and DeMott, P. J.: Single-parameter estimates of aerosol water content, Environ. Res. Lett., 3, 035002 doi:10.1088/1748-9326/3/3/035002, –2008.

Kuwata, M., Kondo, Y., Mochida, M., Takegawa, N., and Kawamura, K.: Dependence of CCN activity of less volatile particles on the amount of coating observed in Tokyo, J. Geophys. Res., 112, D11207, doi:10.1029/2006JD007758, 2007.

~~Kuwata, M., Kondo, Y., Miyazaki, Y., Komazaki, Y., Kim, J. H., Yum, S. S., Tanimoto, H., and Matsueda, H.: Cloud condensation nuclei activity at Jeju Island, Korea in spring 2005, Atmos. Chem. Phys., 8, 2933–2948, doi:10.5194/acp-8-2933-2008, 2008.~~

Lance, S., Medina, J., Smith, J., and Nenes, A.: Mapping the operation of the DMT continuous flow CCN counter, Aerosol Sci. Technol., 40 , 242–254, 2006.

Lathem, T.L., and Nenes, A.: Water vapor depletion in the DMT Continuous Flow CCN Chamber: effects on supersaturation and droplet growth, Aeros.Sci.Tech., **45**, 604–615, doi:10.1080/02786826.2010.551146, 2011.

Lathem, T. L., Beyersdorf, A. J., Thornhill, K. L., Winstead, E. L., Cubison, M. J., Hecobian, A., Jimenez, J. L., Weber, R. J., Anderson, B. E., and Nenes, A.: Analysis

of CCN activity of Arctic aerosol and Canadian biomass burning during summer 2008, Atmos. Chem. Phys., 13, 2735-2756, doi:10.5194/acp-13-2735-2013, 2013.

Lau, K. M., Ramahathan, V., Wu, G., Li, Z., Tsay, S. C., Hsu, C., Sikka, R., Holben, B., Lu,D., Tartari, G., Chin, M., Koudelova, P., Chen, H., Ma, Y., Huang, J., Taniguchi, K., and Zhang, R.: The joint aerosol monsoon experiment: A new challenge for monsoon climate research, Bull. Am. Meteorol. Soc., 89, 369–383, doi:10.1175/BAMS-89-3-369, 2008.

Lee, S. H., Murphy, D. M., Thomson, D. S., and Middlebrook, A. M.: Nitrate and oxidized organic ions in single particle mass spectra during the 1999 Atlanta Supersite Project, J. Geophys. Res., 108, 8417, doi:10.1029/2001JD001455, 2003.

Lee, Y. S., Collins, D. R., Li, R. J., Bowman, K. P., and Feingold, G.: Expected impact of an aged biomass burning aerosol on cloud condensation nuclei and cloud droplet concentrations, J. Geophys. Res., 111, D22204, doi:10.1029/2005JD006464, 2006.

Leng, C., Cheng, T., Chen, J., Zhang, R., Tao, J., Huang, G., Zha, S., Zhang, M., Fang, W., Li, X., Li, L.: Measurements of surface cloud condensation nuclei and aerosol activity in downtown Shanghai. Atmos. Environ., 69, 354-361, 2013.

Liu, J., Zheng, Y., Li, Z., and Cribb, M.: Analysis of cloud condensation nuclei properties at a polluted site in southeastern China during the AMF - China Campaign, J. Geophys. Res., 116, D00K35, doi:10.1029/2011JD016395, 2011.

Li, Z., Chen, H., Cribb, M., Dickerson, R. E., Holben, B., Li, C., Lu, D., Luo, Y., Maring, H., Shi, G., Tsay, S.-C., Wang, P., Wang, Y., Xia, X., Zheng, Y., Yuan, T., and Zhao, F.: Preface to special section on East Asian Studies of Tropospheric Aerosols: An International Regional Experiment (EASTAIRE), J. Geophys. Res., 112, D22S00, doi:10.1029/2007JD008853, 2007a.

Li, Z., Xia, X., Cribb, M., Mi, W., Holben, B., Wang, P., Chen, H., Tsay, S-C., Eck, T. F., Zhao, F., Dutton, E. G., and Dickerson, R. E.: Aerosol optical properties and their radiative effects in northern China, J. Geophys. Res., 112, D22S01, doi:10.1029/ 2006JD007382, 2007b.

Li, Z., Li, C., Chen, H., Tsay, S.-C., Holben, B., Huang, J., Li, B., Maring, H., Qian, Y., Shi, G., Xia, X., Yin, Y., Zheng, Y., and Zhuang, G.: East Asian Studies of Tropospheric Aerosols and Impact on Regional Climate (EAST - AIRC): An overview, J. Geophys. Res., 116, D00K34, doi:10.1029/2010JD015257, 2011.

~~Li, Z.,~~ Liu, J., Zheng, Y., Li, Z., and Cribb, M.: Analysis of cloud condensation nuclei properties at a polluted site in southeastern China during the AMF - China Campaign, J. Geophys. Res., 116, D00K35, doi:10.1029/2011JD016395, 2011.

~~Chen, H., Cribb, M., Dickerson, R. E., Holben, B., Li, C., Lu, D., Luo, Y., Maring, H., Shi, G., Tsay, S.-C., Wang, P., Wang, Y., Xia, X., Zheng, Y., Yuan, T., and Zhao, F.: Preface to special section on East Asian Studies of Tropospheric Aerosols: An International Regional Experiment (EASTAIRE), J. Geophys. Res., 112, D22S00, doi:10.1029/2007JD008853, 2007a.~~

Ma, Y., Brooks, S. D., Vidaurre, G., Khalizov, A. F., Wang, L.: Rapid modification of cloud-nucleating ability of aerosols by biogenic emissions, Geophys. Res. Lett. 40, 6293-6297, doi: 10.1002/2013GL057895, 2013.

~~Mircea, M., Facchini, M. C., Decesari, S., Cavalli, F., Emblico, L., Fuzzi, S., Vestin, A., Rissler, J., Swietlicki, E., Frank, G., Andreae, M. O., Maenhaut, W., Rudich, Y., and Artaxo, P.: Importance of the organic aerosol fraction for modeling aerosol hygroscopic growth and activation: a case study in the Amazon Basin, Atmos. Chem. Phys., 5, 3111–3126, 2005, http://www.atmos-chem-phys.net/5/3111/2005/.~~

Mei, F., Setyan, A., Zhang, Q., and Wang, J.: CCN activity of organic aerosols

observed downwind of urban emissions during CARES, Atmos. Chem. Phys., 13, 12155–12169,doi:10.5194/acp-13-12155-2013, 2013.

Mikhailov, E., Vlasenko, S., Martin, S. T., Koop, T., and P ¨oschl, U.: Amorphous and crystalline aerosol particles interacting with water vapor: conceptual framework and experimental evidence for restructuring, phase transitions and kinetic limitations, Atmos. Chem. Phys., 9, 9491–9522, doi:10.5194/acp-9-9491-2009, 2009.

Mircea, M., Facchini, M. C., Decesari, S., Cavalli, F., Emblico, L., Fuzzi, S., Vestin, A., Rissler, J., Swietlicki, E., Frank, G., Andreae, M. O., Maenhaut, W., Rudich, Y., and Artaxo, P.: Importance of the organic aerosol fraction for modeling aerosol hygroscopic growth and activation: a case study in the Amazon Basin, Atmos. Chem. Phys., 5, 3111–3126, 2005, http://www.atmos-chem-phys.net/5/3111/2005/.

Niedermeier, D., Wex, H., Voigtländer, J., Stratmann, F., Brüggemann, E., Kiselev, A., Henk, H., and Heintzenberg, J.: LACIS-measurements and parameterization of sea-salt particle hygroscopic growth and activation, Atmos. Chem. Phys., 8, 579-590, doi:10.5194/acp-8-579-2008, 2008.

Ng, N. L., Herndon, S. C., Trimborn, A., Canagaratna, M. R., Croteau, P. L., Onasch, T. B., Sueper, D.,Worsnop, D. R., Zhang, Q., Sun, Y. L., and Jayne, J. T.: An Aerosol Chemical Speciation Monitor (ACSM) for Routine Monitoring of the Composition and Mass Concentrations of Ambient Aerosol, Aerosol Sci. Tech., 45, 770–784, 2011.

~~Paramonov, M., Aalto, P. P., Asmi, A., Prisle, N., Kerminen, V.-M., Kulmala, M., and Petäjä, T.: The analysis of size-segregated cloud condensation nuclei counter (CCNC) data and its implications for aerosol-cloud interactions, Atmos. Chem. Phys. Discuss., 13, 9681-9731, doi:10.5194/acpd-13-9681-2013, 2013.~~

带格式的：字体颜色：自动设置

Padró, L. T., Tkacik, D., Lathem, T. L., Hennigan, C. J., Sullivan, A. P., Weber, R. J., Huey, L. G., and Nenes, A.: Investigation of cloud condensation nuclei properties and droplet growth kinetics of the water-soluble aerosol fraction in Mexico City, J. Geophys. Res., 115, D09204, doi:10.1029/2009JD013195, 2010.

Paramonov, M., Aalto, P. P., Asmi, A., Prisle, N., Kerminen, V.-M., Kulmala, M., and Petäjä, T.: The analysis of size-segregated cloud condensation nuclei counter (CCNC) data and its implications for aerosol-cloud interactions, Atmos. Chem. Phys. Discuss., 13, 9681-9731, doi:10.5194/acpd-13-9681-2013, 2013.

Petters, M. D., and Kreidenweis, S. M.: A single parameter representation of hygroscopic growth and cloud condensation nucleus activity, Atmos. Chem. Phys., 7, 1961–1971, doi:10.5194/acp-7-1961-2007, 2007.

Petters, M. D., Carrico, C. M., Kreidenweis, S. M., Prenni, A. J., DeMott, P. J., Collett, J. L., and Moosmu ̈ller, H.: Cloud condensation nucleation activity of biomass burning aerosol, J. Geophys. Res., 114, D22205, doi:10.1029/2009JD012353, 2009.

~~Pringle, K. J., Tost, H., Pozzer, A., Pöschl, U., and Lelieveld, J.: Global distribution of the effective aerosol hygroscopicity parameter for CCN activation, Atmos. Chem. Phys., 10, 5241-5255, doi:10.5194/acp-10-5241-2010, 2010.~~

Quinn, P. K., Bates, T. S., Coffman, D. J., and Covert, D. S.: Influence of particle size and chemistry on the cloud nucleating properties of aerosols, Atmos. Chem. Phys., 8, 1029–1042, 2008, http://www.atmos-chem-phys.net/8/1029/2008/.

Raymond, T. M., and Pandis, S. N.: Cloud activation of single component organic aerosol particles, J. Geophys. Res., 107, 4787, doi:10.1029/2002JD002159, 2002.

Rissler, J., Swietlicki, E., Zhou, J., Roberts, G., Andreae, M. O., Gatti, L. V., and Artaxo, P.: Physical properties of the submicrometer aerosol over the Amazon rain

forest during the wet to dry season transition – comparison of modeled and measured CCN concentrations, Atmos. Chem. Phys., 4, 2119–2143, http://www.atmos-chem-phys.net/4/2119/2004/, 2004.

Roberts, G. C., Artaxo, P., Zhou, J. C., Swietlicki, E., and Andreae, M. O.: Sensitivity of CCN spectra on chemical and physical properties of aerosol: A case study from the Amazon Basin, J. Geophys. Res., 107, 8070, doi:10.1029/2001JD000583, 2002.

Rose, D., Gunthe, S. S., Mikhailov, E., Frank, G. P., Dusek, U., Andreae, M. O., and Poschl, U.: Calibration and measurement uncertainties of a continuous-flow cloud condensation nuclei counter (DMT-CCNC): CCN activation of ammonium sulfate and sodium chloride aerosol particles in theory and experiment, Atmos. Chem. Phys., 8, 1153–1179, 2008, http://www.atmos-chem-phys.net/8/1153/2008/.

Rose, D., Nowak, A., Achtert, P.,Wiedensohler, A., Hu, M., Shao, M., Zhang, Y., Andreae, M. O., and P ¨oschl, U.: Cloud condensation nuclei in polluted air and biomass burning smoke near the mega-city Guangzhou, China – Part 1: Size-resolved measurements and implications for the modeling of aerosol particle hygroscopicity and CCN activity, Atmos. Chem. Phys., 10, 3365–3383, doi:10.5194/acp-10-3365-2010, 2010.

Rose, D., Gunthe, S. S., Su, H., Garland, R. M., Yang, H., Berghof, M., Cheng, Y. F., Wehner, B., Achtert, P., Nowak, A., Wiedensohler, A., Takegawa, N., Kondo, Y., Hu, M., Zhang, Y., Andreae, M. O., and P öschl, U.: Cloud condensation nuclei in polluted air and biomass burning smoke near the mega-city Guangzhou, China – Part 2: Size-resolved aerosol chemical composition, diurnal cycles, and externally mixed weakly CCN-active soot particles, Atmos. Chem. Phys., 11, 2817-2836, doi:10.5194/acp-11-2817-2011, 2011.

~~Rose, D., Gunthe, S. S., Mikhailov, E., Frank, G. P., Dusek, U., Andreae, M. O., and~~

带格式的：字体颜色：自动设置

带格式的：字体颜色：自动设置

带格式的

Poschl, U.: Calibration and measurement uncertainties of a continuous-flow cloud condensation nuclei counter (DMT-CCNC): CCN activation of ammonium sulfate and sodium chloride aerosol particles in theory and experiment, Atmos. Chem. Phys., 8, 1153–1179, 2008, http://www.atmos-chem-phys.net/8/1153/2008/.

Rosenfeld, D., Dai, J., Yu, X., Yao, Z., Xu, X., Yang, X., and Du, C.: Inverse relations between amounts of air pollution and orographic precipitation, Science, 315(5817), 1396–1398, doi:10.1126/science.1137949, 2007.

Salcedo, D., Onasch, T. B., Dzepina, K., Canagaratna, M. R., Zhang, Q., Huffman, J. A., DeCarlo, P. F., Jayne, J. T., Mortimer, P., Worsnop, D. R., Kolb, C. E., Johnson, K. S., Zuberi, B., Marr, L. C., Volkamer, R., Molina, L. T., Molina, M. J., Cardenas, B., Bernabe, R. M., Marquez, C., Gaffney, J. S., Marley, N. A., Laskin, A., Shutthanandan, V., Xie, Y., Brune,W., Lesher, R., Shirley, T., and Jimenez, J. L.: Characterization of ambient aerosols in Mexico City during the MCMA-2003 campaign with Aerosol Mass Spectrometry: results from the CENICA Supersite, Atmos. Chem. Phys., 6, 925–946, 2006.

Sotiropoulou, R. E. P., Nenes, A., Adams, P. J., and Seinfeld, J. H.: Cloud condensation nuclei prediction error from application of K¨ohler theory: Importance for the aerosol indirect effect, J. Geophys. Res., 112, D12202, doi:10.1029/2006JD007834, 2007.

Streets, D. G., Yu, C., Wu, Y., Chin, M., Zhao, Z., Hayasaka, T., and Shi, G.: Aerosol trends over China, 1980–2000, Atmos. Res., 88, 174–182, doi:10.1016/j.atmosres.2007.10.016, 2008.

Stroud, C. A., Nenes, A., Jimenez, J. L., DeCarlo, P., Huffman, J. A., Bruintjes, R., Nemitz, E., Delia, A. E., Toohey, D. W., Guenther, A. B., and Nandi, S.: Cloud Activating Properties of Aerosol Observed during CELTIC, J. Atmos. Sci., 64, 441–

459, 2007.

Sun, Y., Wang, Z., Dong, H., Yang, T., Li, J., Pan, X., Chen, P., and Jayne, J. T.: Characterization of summer organic and inorganic aerosols in Beijing, China with an Aerosol Chemical Speciation Monitor, Atmos. Environ., 51, 250–259, doi:10.1016/j.atmosenv.2012.01.013, 2012.

Takegawa, N., Miyakawa, T., Kawamura, K., and Kondo, Y.: Contribution of selected di-carboxylic and omega-oxocarboxylic acids in ambient aerosol to the m/z 44 signal of an aerodyne aerosol mass spectrometer, Aerosol Sci. Technol., 41, 418–437, doi:10.1080/02786820701203215, 2007.

Turpin, B. J., and Lim, H. J.: Species contributions to PM2.5 mass concentrations: Revisiting common assumptions for estimating organic mass, Aerosol Sci. Tech., 35, 602-610, 2001.

Twomey, S.: Pollution and planetary albedo, Atmos. Environ., 8, 1251–1256, 1974.

~~Twomey, S.: The influence of pollution on the shortwave albedo of clouds, J. Atmos. Sci., 34, 1149–1152, doi:10.1175/1520-0469(1977)034<1149:TIOPOT>2.0.CO;2, 1977.~~

~~VanReken, T. M., Ng, N. L., Flagan, R. C., and Seinfeld, J. H.: Cloud condensation nucleus activation properties of biogenic secondary organic aerosol, J. Geophys. Res., 110, D07206, doi:10.1029/2004JD005465, 2005.~~

VanReken, T. M., Rissman, T. A., Roberts, G. C., Varutbangkul, V., Jonsson, H. H., Flagan, R. C., and Seinfeld, J. H.: Toward aerosol/cloud condensation nuclei (CCN) closure during CRYSTAL-FACE, J. Geophys. Res., 108, 4633, doi:10.1029/2003JD003582, 2003.

VanReken, T. M., Ng, N. L., Flagan, R. C., and Seinfeld, J. H.: Cloud condensation nucleus activation properties of biogenic secondary organic aerosol, J. Geophys.

带格式的

Res., 110, D07206, doi:10.1029/2004JD005465, 2005.

Varutbangkul, V., Brechtel, F. J., Bahreini, R., Ng, N. L., Keywood, M. D., Kroll, J. H., Flagan, R. C., Seinfeld, J. H., Lee, A., and Goldstein, A. H.: Hygroscopicity of secondary organic aerosols formed by oxidation of cycloalkenes, monoterpenes, sesquiterpenes, and related compounds, Atmos. Chem. Phys., 6, 2367–2388, 2006.

Whitby, K., T.: The physical characteristics of sulfur aerosols. Atmos. Environ., 12, 135-159, 1967, Online publication date: 1-Jan-1978, 1978.

Xia, X., Li, Z., Holben, B., Wang, P., Eck, T., Chen, H., Cribb, M., and Zhao, Y.: Aerosol optical properties and radiative effects in the Yangtze Delta region of China, J. Geophys. Res., 112, D22S12, doi:10.1029/2007JD008859, 2007.

Xin, J., Wang, Y., Li, Z., Wang, P., Hao, W., Nordgren, B. L., Wang, S., Liu, G., Wang, L., Wen, T., Sun, Y., Hu, B.: AOD and Angstrom exponent of aerosols observed by the Chinese Sun Hazemeter Network from August 2004 to September 2005, J. Geophys. Res., 112, D05203, doi:10.1029/2006JD007075, 2007.

Xu, Q.: Abrupt change of the mid‐summer climate in central east China by the influence of atmospheric pollution, Atmos. Environ., 35, 5029–5040, doi:10.1016/S1352-2310(01)00315-6, 2001.

Yue, D. L., Hu, M., Zhang, R. J., Wu, Z. J., Su, H., Wang, Z. B., Peng, J. F., He, L.Y., Huang, X. F., Gong, Y. G., and Wiedensohler, A.: Potential contribution of new particle formation to cloud condensation nuclei in Beijing, Atmos. Environ., 45, 6070-6077, 2011.

Yum, S. S., Roberts, G., Kim, J. H., Song, K., and Kim, D.: Submicron aerosol size distributions and cloud condensation nuclei concentrations measured at Gosan, Korea, during the Atmospheric Brown Clouds–East Asian Regional Experiment 2005, J. Geophys. Res., 112, D22S32, doi:10.1029/2006JD008212, 2007.

Zhang, Q., Meng, J., Quan, J., Gao, Y., Zhao, D., Chen, P., and He, H.: Impact of aerosol composition on cloud condensation nuclei activity, Atmos. Chem. Phys., 12, 3783-3790, doi:10.5194/acp-12-3783-2012, 2012.

Zhang, Q., Stanier, C. O., Canagaratna, M. C., Jayne, J. T., Worsnop, D. R., Pandis, S. N., and Jimenez, J. L.: Insights into the Chemistry of New Particle Formation and Growth Events in Pittsburgh Based on Aerosol Mass Spectrometry, Environ. Sci. Technol., 38, 4797–4809, 2004.

Zhang, R., Khalizov, A. F., Pagels, J., Zhang, D., Xue, H., and McMurry, P. H.: Variability in morphology, hygroscopic and optical properties of soot aerosols during internal mixing in the atmosphere, Proc. Natl. Acad. Sci. USA 105, 10291–10296, 2008.

~~Table captions:~~

Tables and Figures

Table 1. ~~Characteristic of~~Parameters describing the CCN efficiency spectra ~~basic spectral parameters~~and hygroscopicity for polluted (*_POL) and background ~~aerosols during~~(*_BG) cases; the ~~campaign for different super saturation. Quantities are midpoint~~ activation ~~diameters~~diameter (D_a~~, D_{cut}~~), the maximum activated ~~fractions~~fraction (MAF), the CDF standard ~~deviations~~deviation (σ), the heterogeneity ~~parameters~~parameter (σ/D_a), and the hygroscopicity ~~parameters~~parameter (κ_a~~, κ_{cut}~~). Values shown are arithmetic mean values with one standard deviation averaged over the entire measurement period.

~~**Figure captions:**~~

SS	D_a_POL	MAF_POL	σ_POL	σ/D_a_POL	κ_a_POL		D_a_BG	MAF_BG	σ_BG	σ/D_a_BG	κ_a_BG
0.08%	190.43±6.11	0.98±0.01	33.34±4.49	0.17±0.02	0.32±0.03		178.68±4.22	0.98±0.01	32.73±2.07	0.18±0.01	0.38±0.02
0.11%	161.80±15.10	0.98±0.01	38.61±7.62	0.22±0.03	0.26±0.05		151.03±2.90	0.97±0.01	28.56±1.97	0.19±0.01	0.33±0.02
0.23%	94.05±8.47	0.96±0.01	27.87±6.30	0.26±0.04	0.31±0.05		91.75±2.48	0.96±0.00	18.81±1.53	0.20±0.01	0.34±0.02
0.42%	63.33±3.65	0.94±0.01	18.02±2.84	0.26±0.03	0.30±0.04		64.06±1.24	0.95±0.00	16.21±0.81	0.25±0.01	0.29±0.01
0.80%	44.78±2.51	0.94±0.01	14.08±0.98	0.29±0.01	0.24±0.03		45.67±1.29	0.95±0.01	13.82±1.17	0.30±0.02	0.22±0.02

带格式的
带格式的：行距：单倍行距
带格式的：字体颜色：黑色
带格式的
带格式的
带格式的

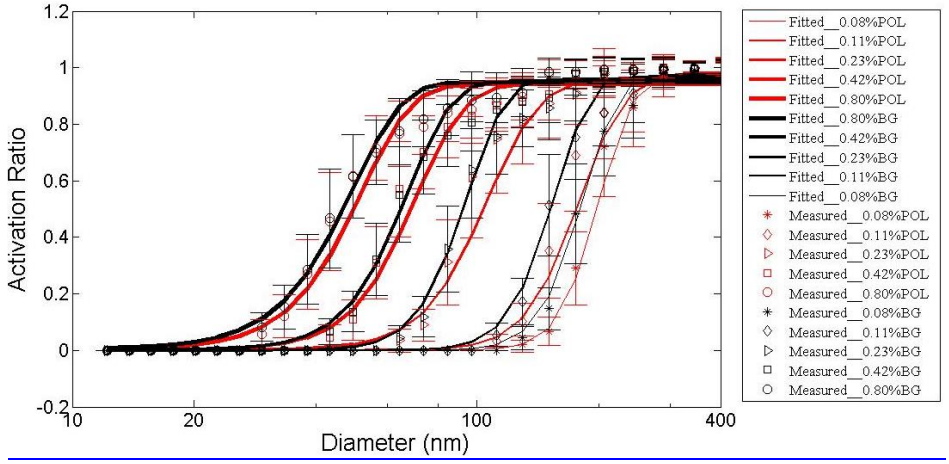

Fig. 1. Averaged measured and fitted CCN efficiency spectra ~~by~~from the 3-parameter CDF fit at SS ~~of~~= 0.08%, 0.11%, 0.23%, 0.42~~%~~%, and 0.80% ~~for~~under polluted (Pol) and background (BG) conditions during the size-resolved CCN ~~measurements~~measurement period.

带格式的：行距：1.5 倍行距

带格式的：字体：（国际）Times New Roman

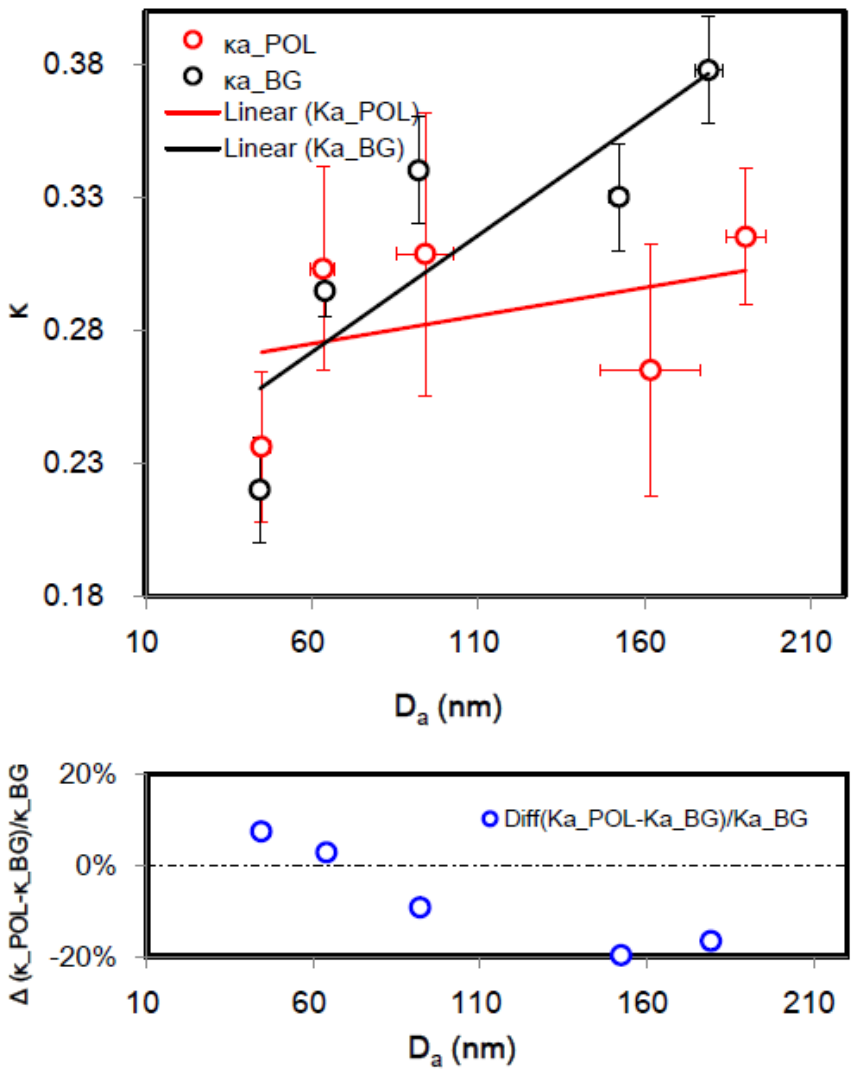

Fig. 2. **Top:** Derived hygroscopicity ~~parameters~~parameter, κ_a ~~against the~~, as a function of particle ~~diameters for~~ diameter, D_a, under polluted (POL) and background (BG) conditions. **Bottom:** Percent ~~changes of~~change in κ_a due to ~~the pollutions are plotted here.~~ pollution as a function of D_a. Error bars represent one standard deviation calculated over the entire measurement period.

带格式的：行距：1.5 倍行距

带格式的：字体：加粗

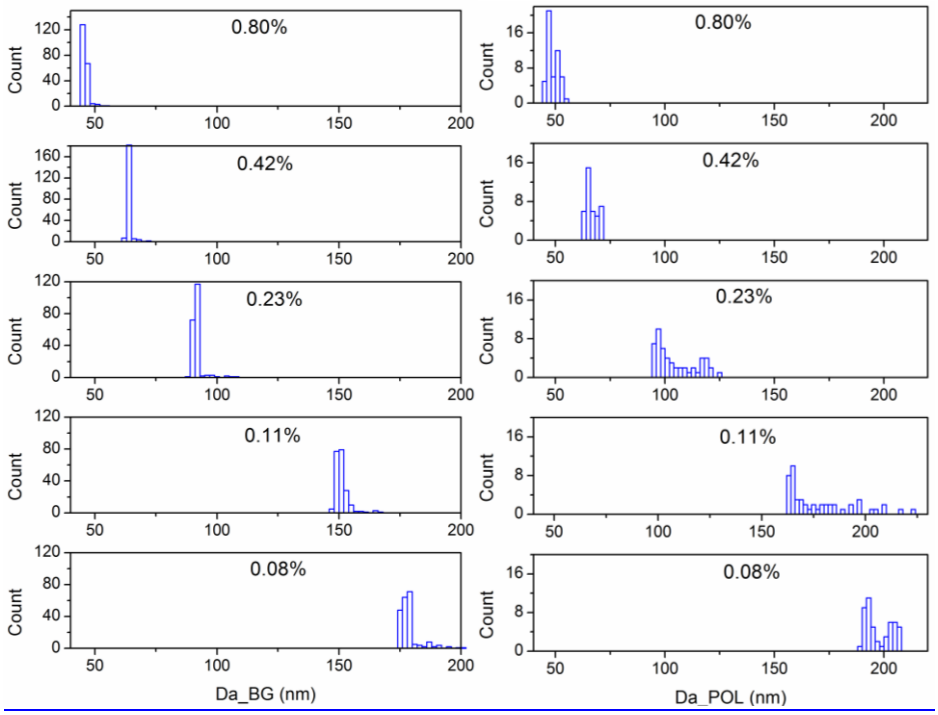

Fig. 3. Probability distribution ~~(PDF)~~functions of D_a under background and polluted conditions at five SS ~~of~~ levels (0.08-0.80~~%~~%) during the size-resolved CCN ~~measurements~~measurement period.

带格式的：行距：1.5 倍行距

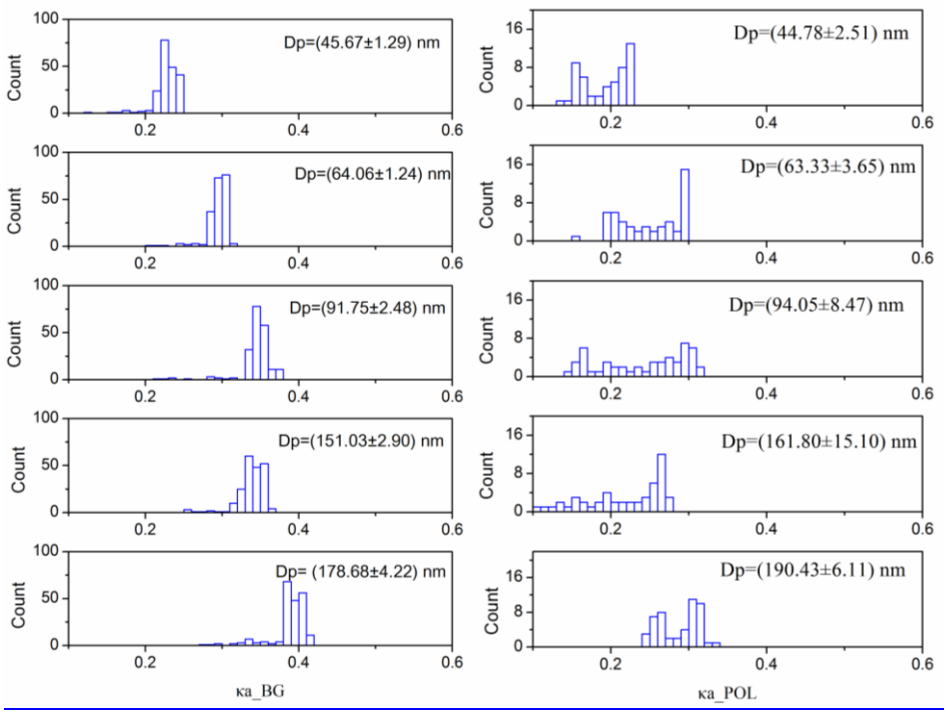

Fig. 4 ~~PDF.~~ Probability distribution functions of $\kappa_{\text{~~cut~~a}}$ under background (left panels) and polluted (right panels) conditions ~~at~~for different particle size ranges during the size-resolved CCN ~~measurements~~measurement period.

带格式的：行距：1.5 倍行距

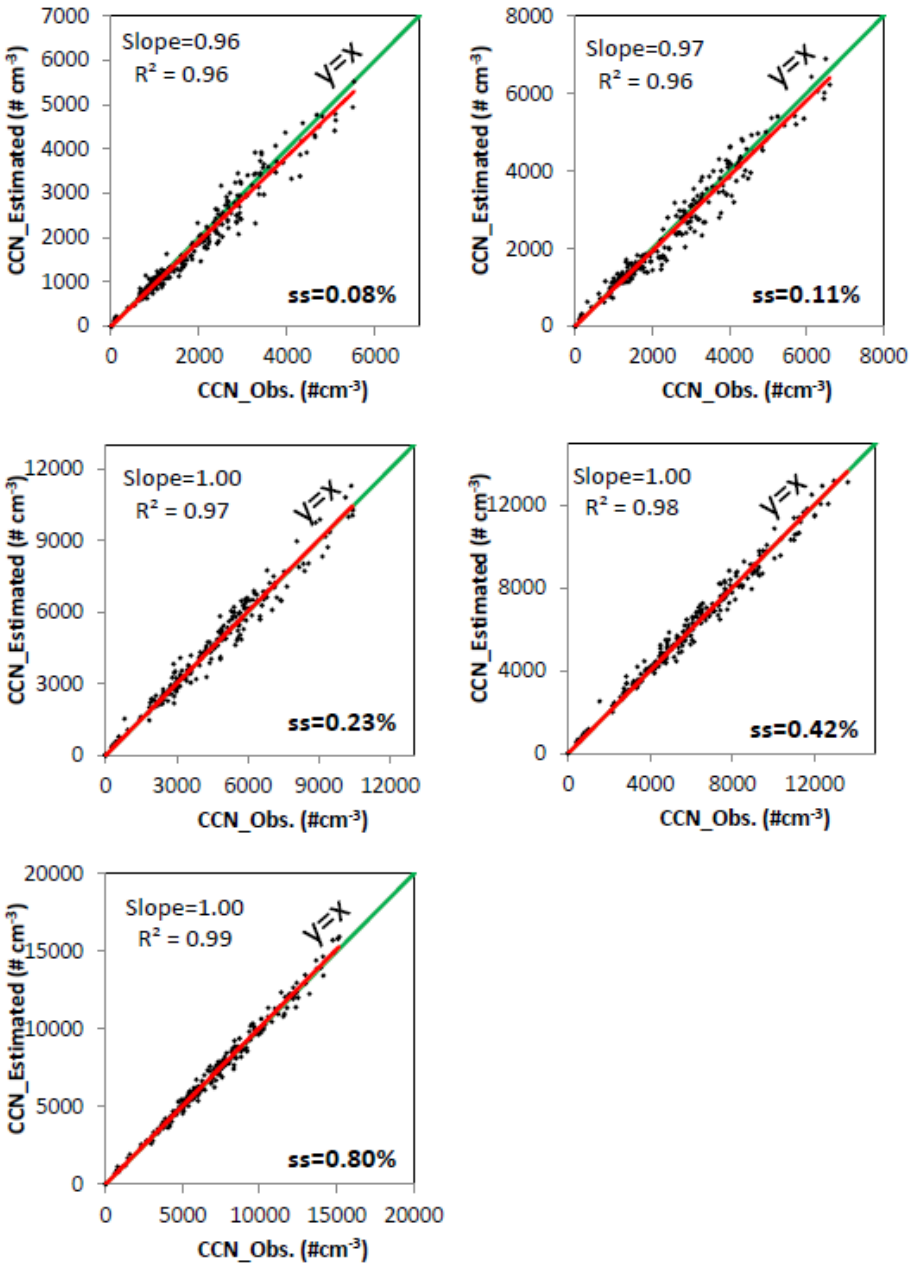

Fig. 5. Estimated N_{CCN} ~~plotted against the~~ as a function of observed N_{CCN} ~~in~~at different SS levels in the parallel observation (PO) closure test. The green solid line is the 1:1 line.

带格式的：行距：1.5 倍行距

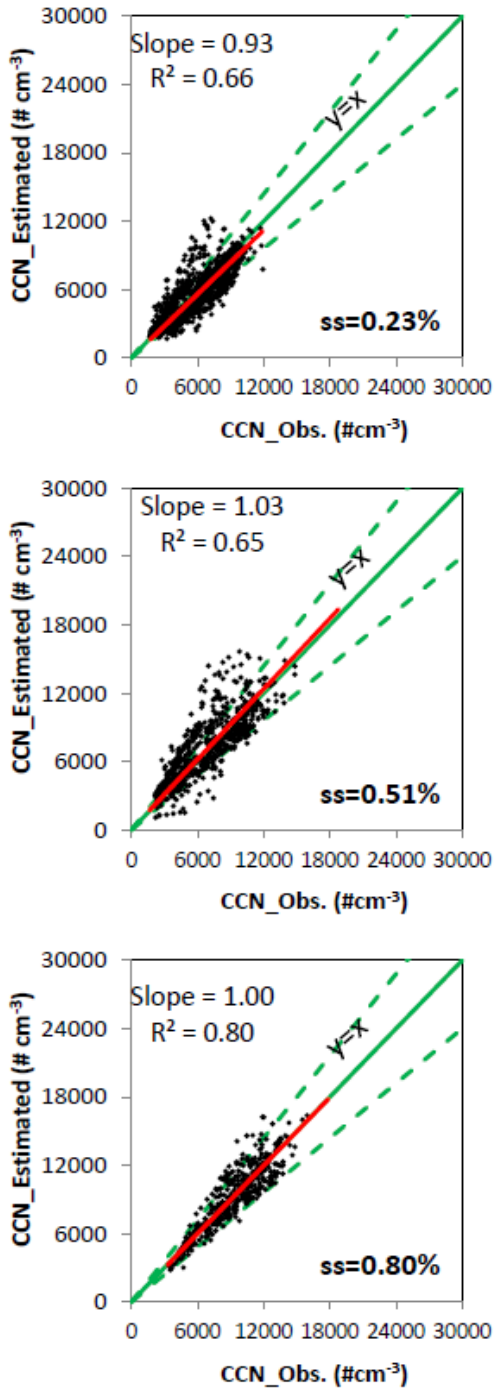

Fig. 6. As in Figure 5, but for the non~~Fig. 6 Estimated N_{CCN} plotted against the observed N_{CCN} in Non~~-parallel observation (NPO) closure test. The ~~green solid line is the 1:1 line, and the~~ dashed green lines indicate the ~~band of about~~boundaries

带格式的: 行距: 1.5 倍行距

representing ±30% ~~deviation~~deviations of N_{CCN}-estimated from N_{CCN}-observed.

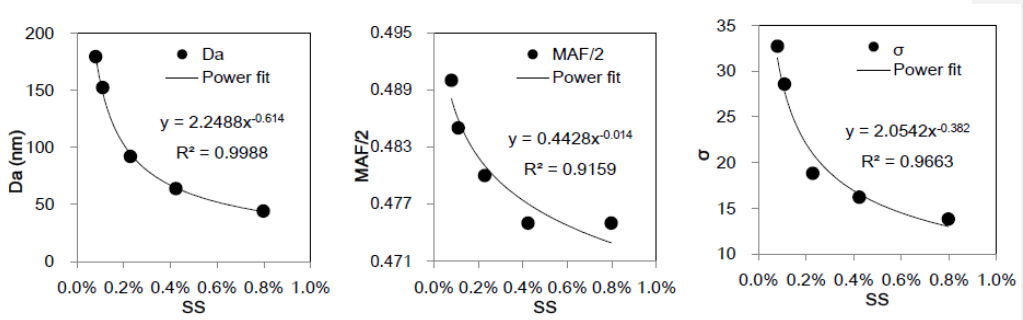

Fig. 7. D_a, MAF, and σ as a function of SS.

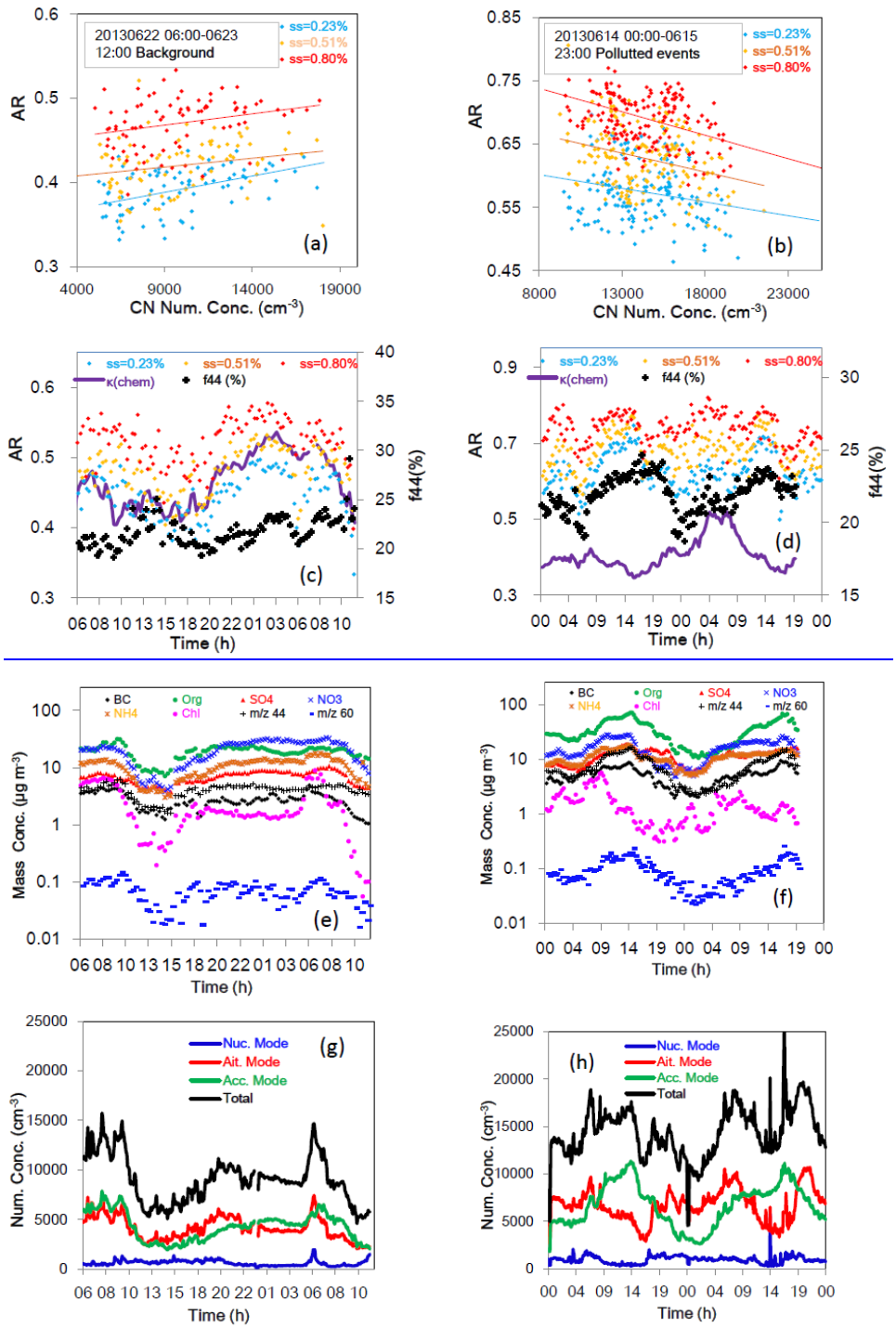

Fig. ~~7 Two selected cases of~~8. Measurements made under background conditions (22-23 June~~,~~ 2013~~) with,~~ N_{CN} of < 15000 cm^{-3} ~~(left)~~ and polluted ~~events~~conditions (14-15 June~~,~~ 2013~~) with,~~ N_{CN} of > 15000 cm^{-3} ~~(right) during the campaign.~~). Bulk

带格式的：字体：加粗

带格式的：行距：1.5 倍行距

CCN activation ratios ~~(AR)~~ at ~~all three supersaturations of~~ SS = 0.2%, 0.5~~%~~%, and 0.8% ~~against~~ as a function of N_{CN} ~~in clear days~~ under background and polluted ~~days~~conditions are shown in Fig~~7a~~. 8a and Fig. ~~7b~~8b, respectively. Diurnal variations ~~of~~in AR, derived from κ_{chem} and the fraction of total organic mass signal at ~~*m/z* 44 (~~f44~~) are shown in Fig. 7c (~~, under background and polluted conditions~~) and~~ are shown in Fig. ~~7d (polluted events).~~8c and Fig. 8d, respectively. Mass concentrations of black carbon (BC), organics, nitrate (NO_3^-), ammonium (NH_4^+), sulfate (SO_4^{2-}), chloride (Cl^-) ~~ions~~ions, etc~~. are shown in Fig. 7e (~~., under background and polluted conditions~~)~~ are shown in Fig. 8e and Fig.~~7f (polluted events).~~ 8f, respectively. N_{CN} ~~at size range of~~ for nucleation~~,~~ (10-30 nm), Aitken ~~and accumulated mode are shown in Fig 7g and Fig. 7h for~~ (30-130 nm), and accumulation modes (130-700 nm) under background ~~conditions~~ and polluted ~~events~~conditions are shown in Fig. 8g and Fig. 8h, respectively.

带格式的
带格式的
带格式的
带格式的
带格式的
带格式的

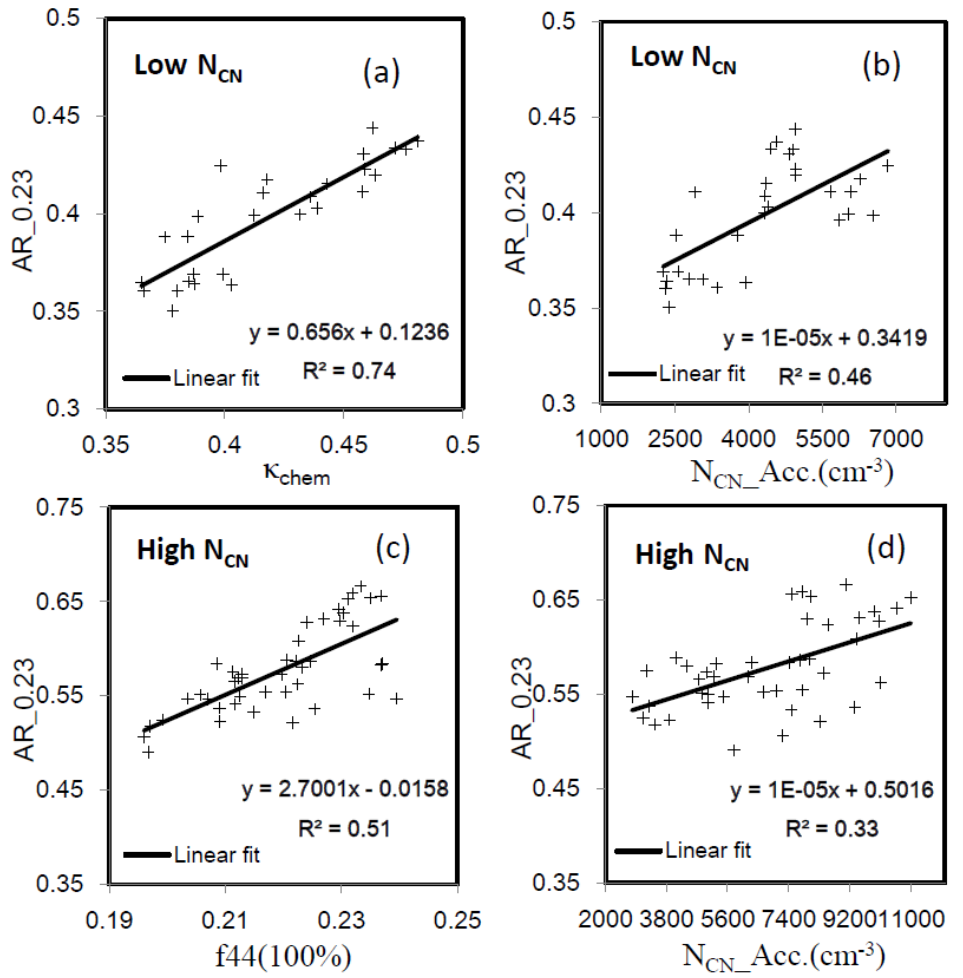

Fig. ~~8 Correlations~~9. AR measured at SS = 0.23% as a function of ~~AR with~~(a) κ_{chem}, ~~$f44$ and N_{CN}_Acc. at~~ under background ~~(with low N_{CN}) and~~conditions, (b) accumulation mode N_{CN} under background conditions, (c) f_{44} under polluted ~~(with high N_{CN}) cases.~~conditions, and (d) accumulation mode N_{CN} under polluted conditions. The ~~AR~~accumulation mode size range is ~~measured at SS=0.2%, the N_{CN}_Acc. is CN number concentrations at accumulated modes.~~130-700 nm in this study.

带格式的：缩进：左侧： 0 厘米，悬挂缩进：1 字符，首行缩进： -1 字符，定义网格后不调整右缩进，行距：1.5 倍行距，不调整西文与中文之间的空格，不调整中文和数字之间的空格

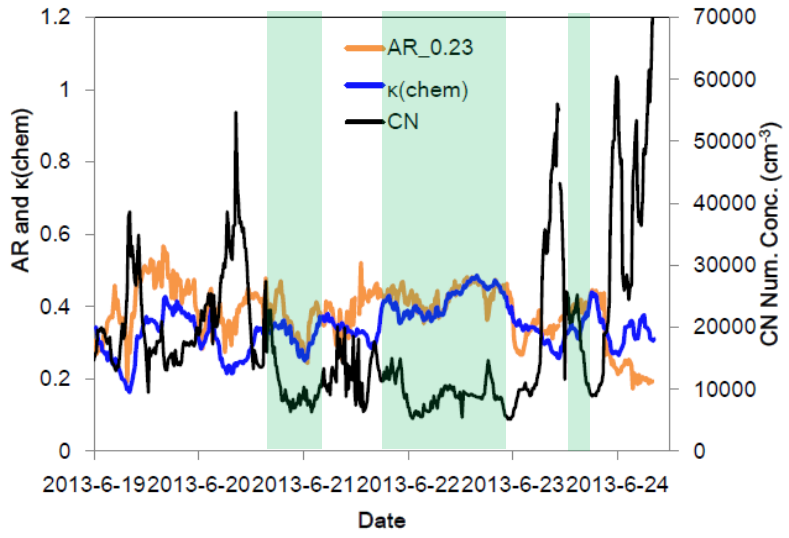

Fig. ~~**9. An example for temporal variations**~~**10.** Time series of bulk AR at ~~supersaturation of~~SS = 0.~~5~~23%, derived κ_{chem}, and N_{CN} ~~during the campaign (~~from 19-24 June~~,~~ 2013~~). The~~. Green shaded areas highlight periods ~~(with low N_{CN})~~ when there was a high correlations between bulk AR and κ_{chem} ~~were observed were marked by rectangles in light green color~~.

带格式的: 行距: 1.5 倍行距

带格式的: 字体: 小四

带格式的: 字体: Times New Roman, 小四

带格式的

带格式的: 缩进: 左侧: 0 厘米, 首行缩进: 0 字符, 定义网格后自动调整右缩进, 调整中文与西文文字的间距, 调整中文与数字的间距

Table 1. Characteristic of spectra basic spectral parameters for polluted and background aerosols during the campaign for different super saturation. Quantities are midpoint activation diameters (D_a, D_{cut}), maximum activated fractions (MAF), CDF standard deviations (σ), heterogeneity parameters (σ/D_a), hygroscopicity parameters (κ_a, κ_{cut}).

SS	D_a_POL	D_{cut}_POL	MAF_POL	σ_POL	σ/D_a_POL	κ_a_POL	κ_{cut}_POL	—	D_a_BG	D_{cut}_BG	MAF_BG	σ_BG	σ/D_a_BG	κ_a_BG	κ_{cut}_BG
0.079%	190.43±6.11	191.27±5.23	0.98±0.01	33.34±4.49	0.17±0.02	0.32±0.03	0.31±0.02		178.68±4.22	180.22±3.97	0.98±0.01	32.73±2.07	0.18±0.01	0.38±0.02	0.37±0.03
0.109%	161.80±15.10	162.93±15.14	0.98±0.01	38.61±7.62	0.22±0.03	0.26±0.05	0.26±0.05		151.03±2.90	153.62±2.69	0.97±0.01	28.56±1.97	0.19±0.01	0.33±0.02	0.31±0.02
0.228%	94.05±8.47	95.31±7.01	0.96±0.01	27.87±6.30	0.26±0.04	0.31±0.05	0.30±0.05		91.75±2.48	93.40±2.27	0.96±0.00	18.81±1.53	0.20±0.01	0.34±0.02	0.32±0.02
0.423%	63.33±3.65	64.76±3.14	0.94±0.01	18.02±2.84	0.26±0.03	0.30±0.04	0.28±0.04		64.06±1.24	65.86±1.13	0.95±0.00	16.21±0.81	0.25±0.01	0.29±0.01	0.27±0.02
0.797%	44.78±2.51	47.55±2.65	0.94±0.01	14.08±0.98	0.29±0.01	0.24±0.03	0.20±0.04	—	45.67±1.29	47.25±1.16	0.95±0.01	13.82±1.17	0.30±0.02	0.22±0.02	0.20±0.02

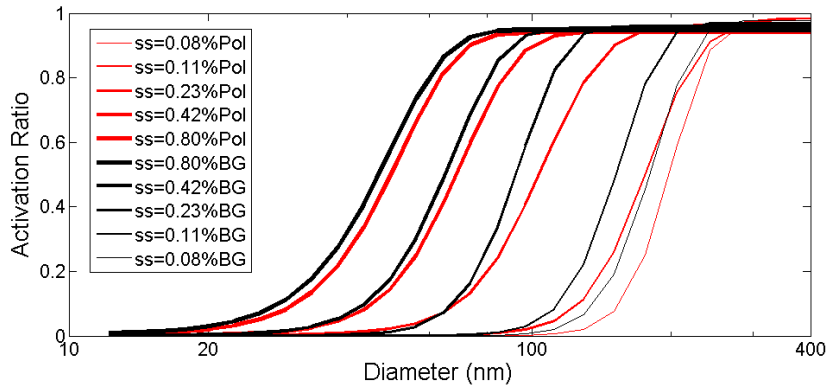

~~Fig. 1.~~ ~~Averaged measured CCN efficiency spectra by the 3-parameter CDF fit at SS of 0.08%, 0.11%, 0.23%, 0.42% and 0.80% for polluted and background conditions during the size-resolved CCN measurements period.~~

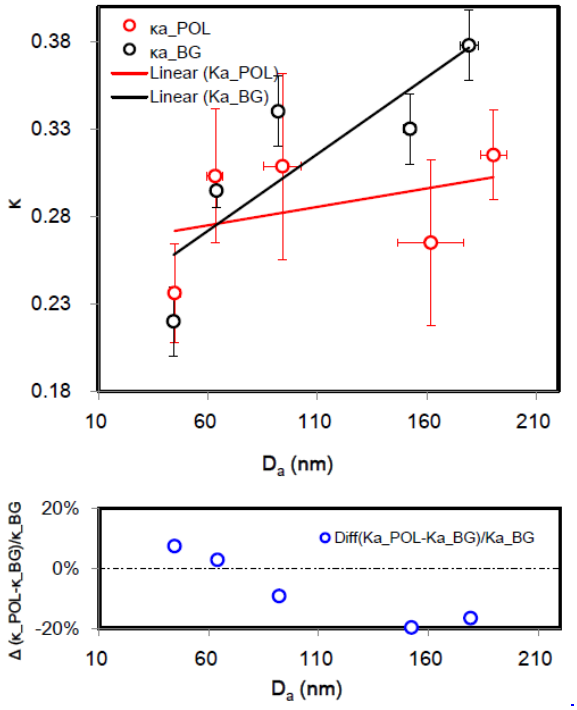

~~**Fig. 2.** Derived hygroscopicity parameters, κ_a against the particle diameters for polluted and background conditions. Percent changes of κ_a due to the pollutions are plotted here.~~

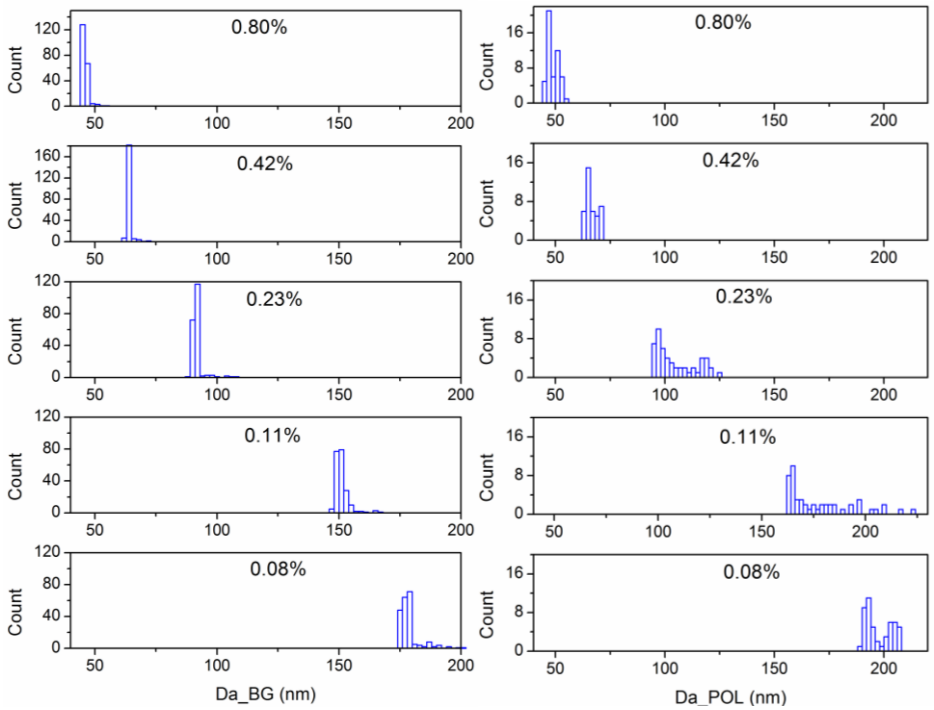

~~Fig. 3~~ ~~Probability distribution (PDF) of D_a under background and polluted conditions at five SS of 0.08-0.80% during the size-resolved CCN measurements period.~~

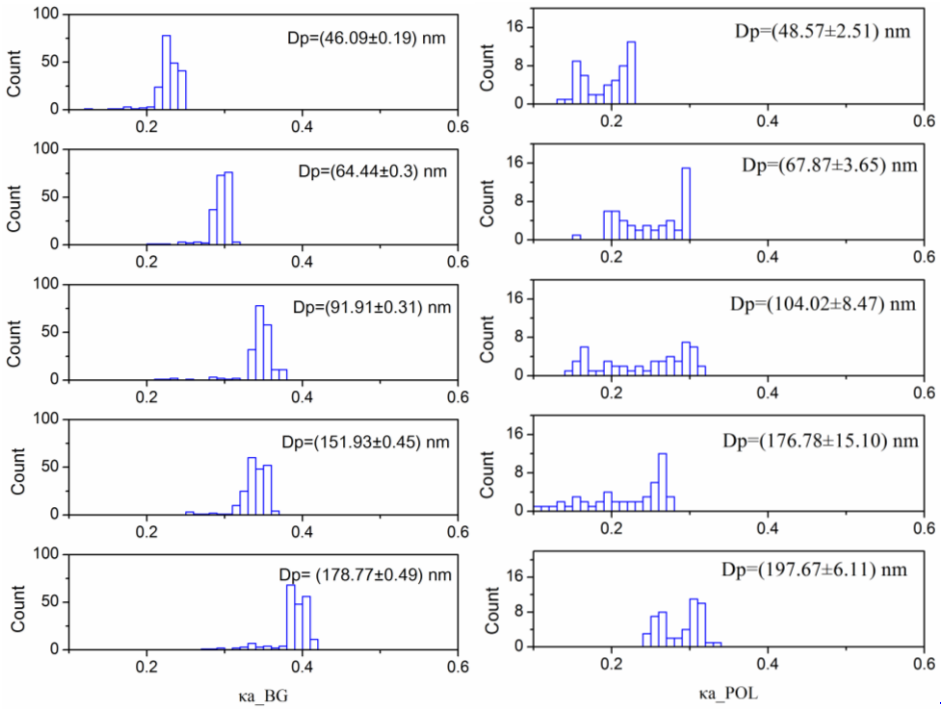

Fig. 4 PDF of κ_{cut} under background and polluted conditions at different particle size ranges during the size-resolved CCN measurements period.

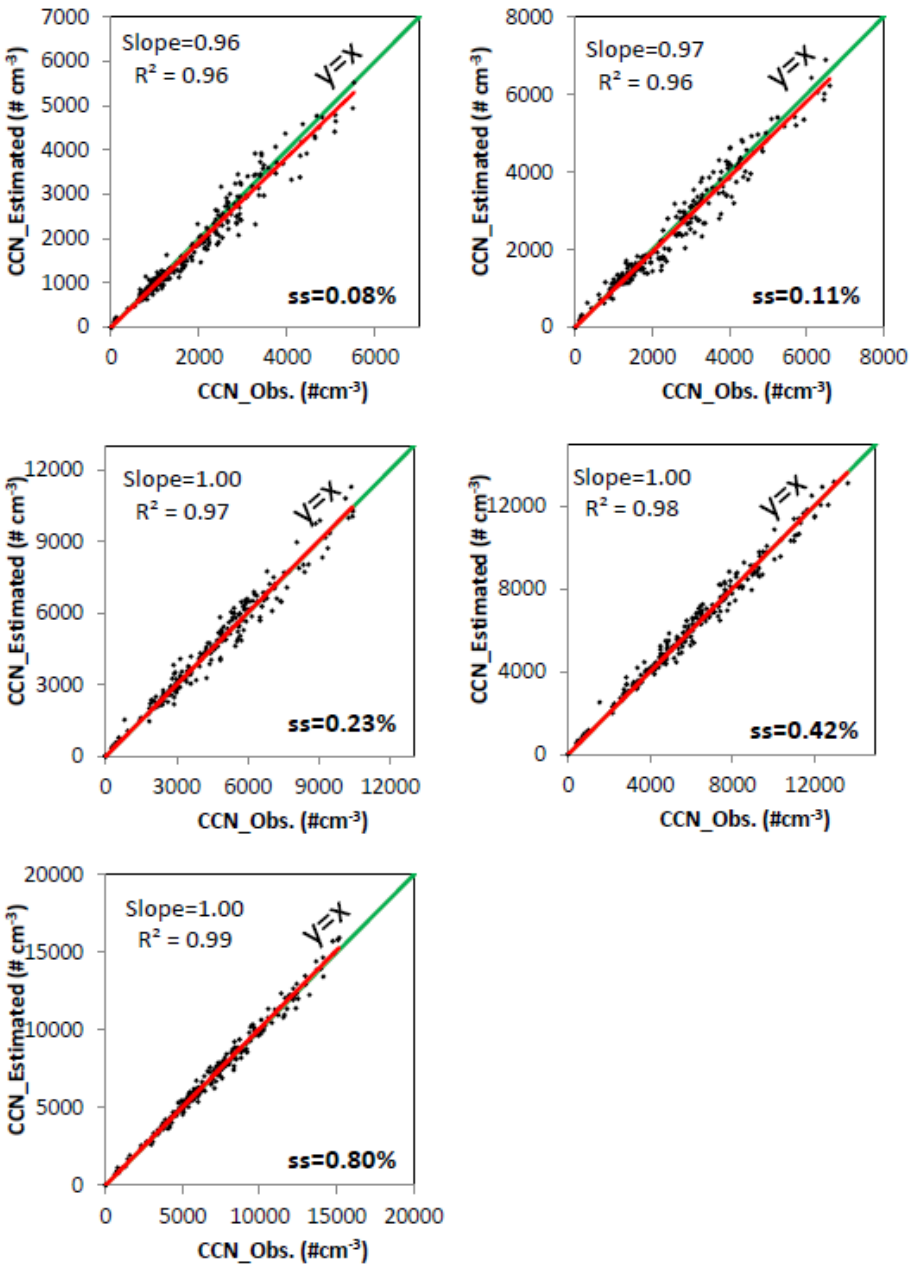

Fig. 5 Estimated N_{CCN} plotted against the observed N_{CCN} in parallel observation (PO) closure test. The green solid line is the 1:1 line.

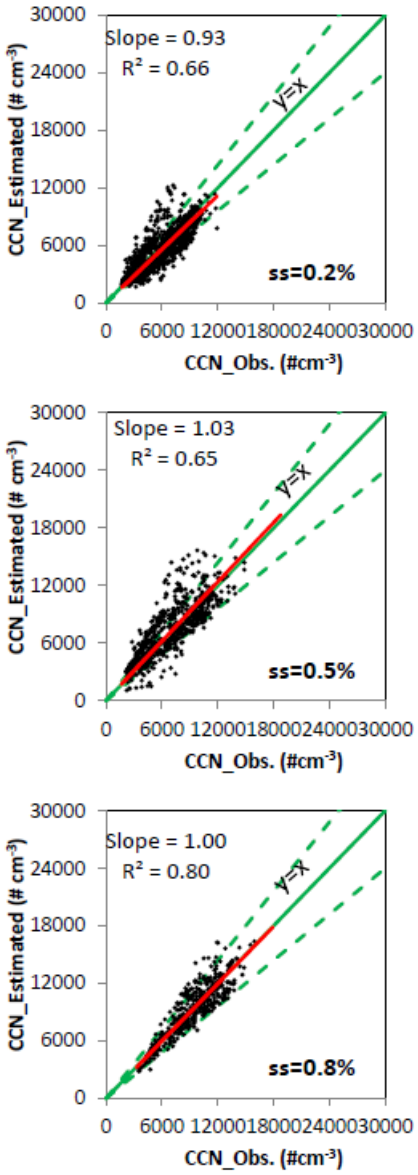

~~Fig. 6~~ ~~Estimated N_{CCN} plotted against the observed N_{CCN} in Non-parallel observation (NPO) closure test. The green solid line is the 1:1 line, and the dashed green lines indicate the band of about ±30% deviation of N_{CCN} estimated from N_{CCN} observed.~~

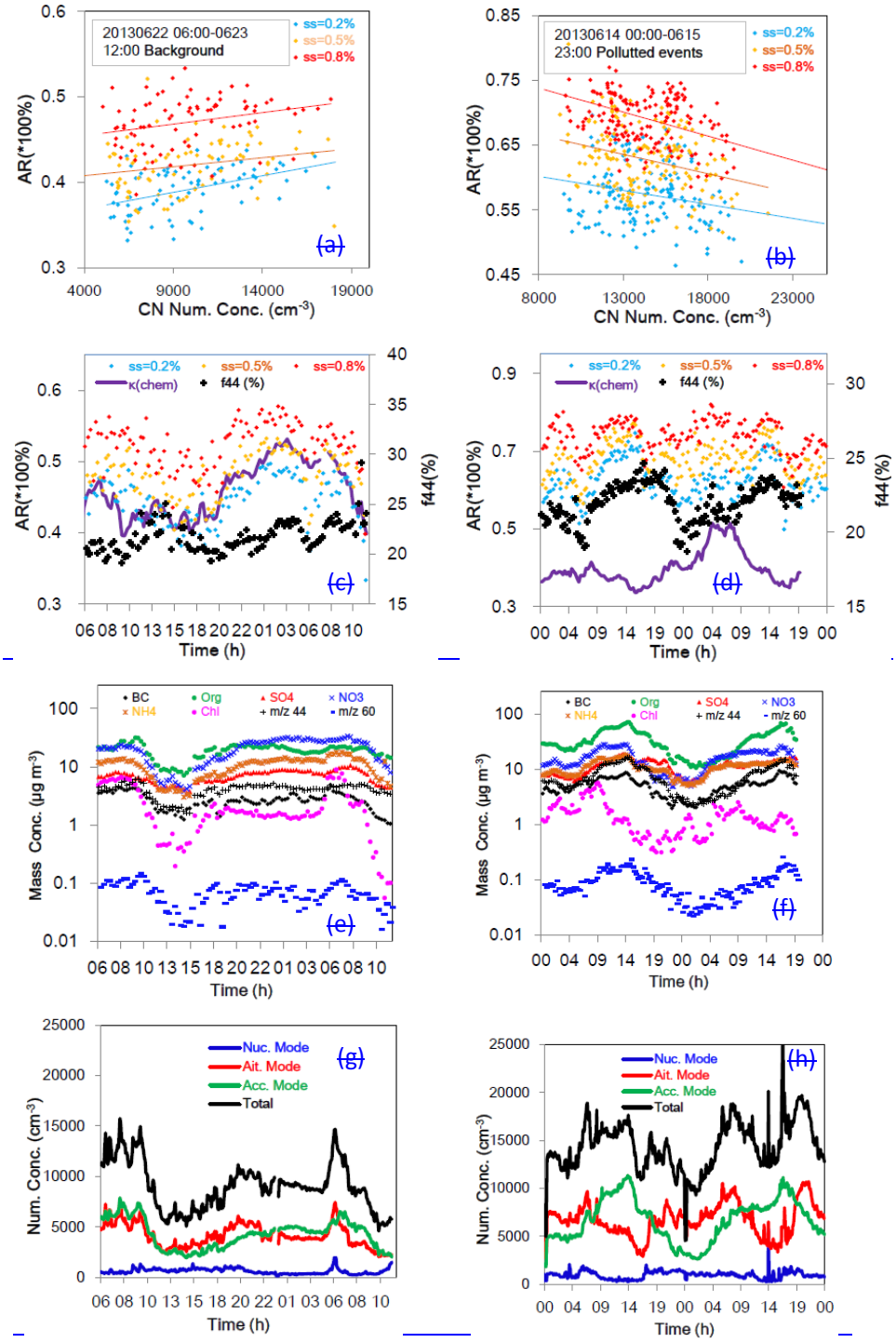

~~**Fig. 7** Two selected cases of background conditions (22-23 June, 2013) with N_{CN} of <15000 cm^{-3} (left) and polluted events (14-15 June, 2013) with N_{CN} > 15000 cm^{-3} (right) during the campaign. Bulk CCN activation ratios (AR) at all three~~

supersaturations of 0.2%, 0.5% and 0.8% against N_{CN} in clear days and polluted days are shown in Fig 7a and Fig. 7b respectively. Diurnal variations of AR, derived κ_{chem} and fraction of total organic mass signal at *m/z* 44 (f44) are shown in Fig. 7c (background conditions) and Fig. 7d (polluted events). Mass concentrations of black carbon (BC), organics, nitrate (NO_3^-), ammonium (NH_4^+), sulfate (SO_4^{2-}), chloride (Cl^-) irons etc. are shown in Fig. 7e (background conditions) and Fig.7f (polluted events). N_{CN} at size range of nucleation, Aitken and accumulated mode are shown in Fig 7g and Fig. 7h for background conditions and polluted events respectively.

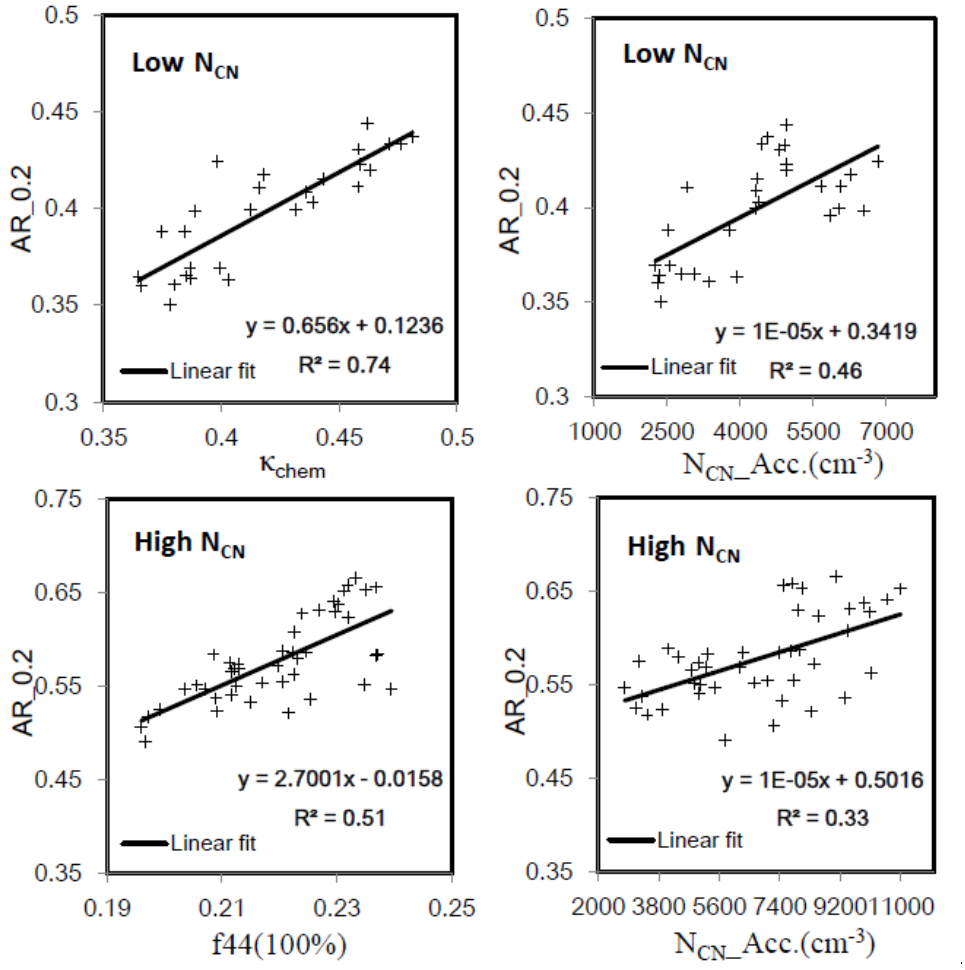

Fig. 8 Correlations of AR with κ_{chem}, *f*44 and N_{CN}_Acc. at background (with low N_{CN}) and polluted (with high N_{CN}) cases. The AR is measured at SS=0.2%, the N_{CN}_Acc. is CN number concentrations at accumulated modes.

~~**Fig. 9.** An example for temporal variations of bulk AR at spersaturation of 0.5%, derived κ_{chem} and N_{CN} during the campaign (19-24 June, 2013). The periods (with low N_{CN}) when high correlations between bulk AR and κ_{chem} were observed were marked by rectangles in light green color.~~

带格式的：字体：小四